# THEORETICAL AND LABORATORY STUDIES ON THE INTERACTION OF COSMIC-RAY PARTICLES WITH INTERSTELLAR ICES. III. SUPRATHERMAL CHEMISTRY–INDUCED FORMATION OF HYDROCARBON MOLECULES IN SOLID METHANE ($CH_4$), ETHYLENE ($C_2H_4$), AND ACETYLENE ($C_2H_2$)

R. I. KAISER[1] AND K. ROESSLER[2]

## ABSTRACT

Methane, ethylene, and acetylene ices are irradiated in a ultra high vacuum vessel at 10 K with 9.0 MeV $\alpha$-particles and 7.3 MeV protons to elucidate mechanisms to form hydrocarbon molecules upon interaction of Galactic cosmic-ray particles with extraterrestrial, organic ices. Theoretical calculations focus on computer simulations of ion-induced collision cascades in irradiated targets. Our experimental and computational investigations reveal that each MeV particle transfers its kinetic energy predominantly through inelastic encounters to the target leading to electronic excitation and ionization of the target molecules. Here electronically excited $CH_4$ species can fragment to mobile H atoms and nonmobile $CH_3$ radicals. The potential energy stored in Coulomb interaction of the $CH_4^+$ ions release energetic H and C atoms not in thermal equilibrium with the 10 K target (suprathermal species). Moderated to 1–10 eV kinetic energy, these carbon atoms and those triggered by the elastic energy transfer of the MeV projectile to the target are found to abstract up to two H atoms to yield suprathermal CH and $CH_2$ species. C and CH, as well as $CH_2$, can insert into a C—H bond of a $CH_4$ molecule to form methylcarbene ($HCCH_3$), the ethyl radical ($C_2H_5$), and ethane ($C_2H_6$). $HCCH_3$ either loses $H_2/2H$ to form acetylene, $C_2H_2$, rearranges to ethylene, $C_2H_4$, or adds two H atoms to form ethane, $C_2H_6$. $C_2H_5$ can abstract or lose an H atom, giving ethane and ethylene, respectively. $C_2H_2$ and $C_2H_4$ are found to react with suprathermal H atoms to form $C_2H_3$ and $C_2H_5$, respectively. Overlapping cascades and an increasing MeV ion exposure transforms $C_2H_x$ ($x = 2, \ldots, 6$) to even more complex alkanes up to $C_{14}H_{30}$. These elementary reactions of suprathermal species to insert, abstract, and add in/to bonds supply a powerful pathway to form new molecules in icy grain mantles condensed on interstellar grains or in hydrocarbon rich bodies in our solar system even at temperatures as low as 10 K.

*Subject headings:* cosmic rays — ISM: molecules — methods: laboratory — molecular processes

## 1. INTRODUCTION

The interstellar medium (ISM) contains $\approx 10\%$ of the mass of our Galaxy and consists of gas (99%) as well as 0.1–0.2 $\mu$m ellipsoidal-shaped grain particles (1%), with averaged number densities of 1 H atom $cm^{-3}$ and $10^{-11}$ grains $cm^{-3}$, respectively (Hollenbach & Thronson 1987). Its chemical composition is dominated by hydrogen and helium (93.38% H, 6.49% He), whereas oxygen, carbon, and nitrogen contribute only 0.11% (O:C:N $\approx$ 6:3:1) (Scheffler & Elsässer 1988; Cowley 1985). The remaining elements furnish 0.02%. This elementary composition is reflected in 106 hitherto identified detected interstellar radicals, atoms, and molecules as well. These species are not spread homogeneously in the interstellar medium (ISM) but disclose pronounced localization in large-scale structures such as interstellar clouds and more localized circumstellar envelopes of, e.g., dying carbon and oxygen stars. Diffuse (hot) clouds hold number densities of $n$ of about 10 mol $cm^{-3}$ and mean translational temperatures $T$ of 100 K, while in dense (cold, dark, molecular) clouds typical scenarios range $n = 10^2$–$10^6$ $cm^{-3}$ and $T = 10$–40 K. Molecules in the outflow of carbon stars contribute only a minor amount to the interstellar matter, but temperatures can rise up to 4000 K in the outer photosphere (Alksne, Alksnis, & Dzervitis 1991), and a more complex chemistry is anticipated.

Although the interstellar dust component embodies only 1% of the ISM mass, these predominantly silicate- and carbonaceous-based grain nuclei play a key role in the formation of new molecules (Hollenbach & Thronson 1987). Deep in the interior of dense molecular clouds, grain particles effectively shield newly synthesized molecules in the gas phase from the destructive external Galactic UV radiation field with a flux $\phi$ of about $10^8$ photons $cm^{-2}$ $s^{-1}$ at energies greater than 6.2 eV. In addition, these grains hold typical temperatures of 10 K in molecular clouds (Greenberg 1971; Tielens & Allamandola 1987) and molecules, radicals as well as atoms from the gas phase are accreted on grain surfaces resulting in an icy mantle up to 0.1 $\mu$m thick. Here solid mixtures containing $H_2O$, CO, $CH_3OH$, $NH_3$, $H_2S$, $CH_4$, $H_2CO$, OCS, $OCN^-$, $H_2$, and $CO_2$ were identified unambiguously via IR spectroscopy on interstellar grains (Whittet 1993; Schmitt 1994; Schutte 1998; Tielens et al. 1991b; Chiar et al. 1994; Grim & Greenberg 1987; Lacy et al. 1984; Tegler et al. 1995; Schutte et al. 1996; Palumbo, Tielens, & Tokunaga 1995; Schutte & Greenberg 1997). Further, molecular hydrogen, $H_2$, the most abundant interstellar molecule, is thought to be formed predominantly on grain surfaces via recombination of two physi-/chemisorbed H atoms (Tielens & Allamondola 1987) and inside ice layers thru suprathermal chemistry (Kaiser et al. 1997).

[1] Institut für Nuklearchemie, Forschungszentrum Jülich, 52425 Jülich, Germany. Present address: Institute of Atomic and Molecular Sciences, 1, Section 4, Roosevelt Road, Taipei, 106, Taiwan; kaiser@po.iams.sinica.edu.tw.

[2] Institut für Nuklearchemie, Forschungszentrum Jülich, 52425 Jülich, Germany.

This ice mantle is processed by the cosmic-ray-induced internal UV radiation present even in the deep interior of dense clouds ($\phi = 10^3$ photons cm$^{-2}$ s$^{-1}$) (d'Hendecourt & Allamandola 1986; Allamandola, Sandford, & Valero 1988; Grim et al. 1989; Shalabiea & Greenberg 1994) and through particles of the Galactic cosmic radiation field, leading to new molecules synthesized in the solid state (Johnson, Lanzerotti, & Brown 1984; Geiss et al. 1992; Simpson 1983; Johnson 1990; Brown, Lanzerotti, & Johnson 1982). The particle component consists of 97%–98% protons ($p$, H$^+$) and 2%–3% helium nuclei ($\alpha$-particles, He$^{2+}$) in the low-energy range of 1–10 MeV, with $\phi = 10$ particles cm$^{-2}$ s$^{-1}$ (Johnson 1990; Lanzerotti & Johnson 1987) and higher energies up to the PeV limit ($\phi = 10^{-12}$ particles cm$^{-2}$ s$^{-1}$). Since, however, typical carbon-hydrogen and carbon-carbon bond strengths in organic molecules range between 3 and 10 eV, the cosmic-ray particles are too energetic to form stable chemical bond as implanted into the icy mantle. But upon interaction with the solid target, each cosmic-ray particle releases its excess energy to the target atoms in successive collisions via elastic and inelastic interactions (Kaiser & Roessler 1997). Here the elastic process transfers energy to the nuclei of the target atoms igniting *primary knock-on particles* (PKOs; first generation of knock-on particles) if this amount is larger than the binding energy of the atom. MeV $\alpha$-particles, for example, generate carbon PKOs with kinetic energies up to 10 keV. These knock-on particles can transfer their energy in consecutive encounters to the target atoms resulting in a collision cascade of secondary, tertiary, etc., knock-on atoms. Moderated to about 1–10 eV, the so-called chemical energy range, these atoms are not in thermal equilibrium with the 10 K target (hence: nonequilibrium or suprathermal particles) and can react finally with the target molecules via elementary steps of bond insertion, addition to double or triple bonds, or hydrogen abstraction (Stöcklin 1969; Roessler 1991).

The power of these suprathermal reactions to form new molecules at temperatures even as low as 10 K is based in their ability to overcome reaction barriers in the entrance channel easily since suprathermal species can impart their excess kinetic energy into the transition state of the reaction. Even reactions endothermic at 10 K are feasible and extend the synthetic power of this reaction class further beyond thermal processes of diffusion controlled chemistry on interstellar grains (Roessler 1991). These unique aspects of suprathermal reactions result in reaction rate constants $k$ orders of magnitude larger than their thermal counterparts. Detailed calculations on the reactions of, e.g., 1 eV suprathermal hydrogen atoms with H$_2$O and CH$_4$ to form H$_2$ and OH as well as CH$_3$, respectively, depict $k$ (1 eV H, H$_2$O) = $1.7 \times 10^{-11}$ cm$^3$ s$^{-1}$ and $k$ (1 eV H, CH$_4$) = $5.0 \times 10^{-11}$ cm$^3$ s$^{-1}$ versus thermal rate constants of $k$ (293 K, H + H$_2$O) = $9.6 \times 10^{-27}$ cm$^3$ s$^{-1}$ and $k$ (293 K, H + CH$_4$) = $2.5 \times 10^{-19}$ cm$^3$ s$^{-1}$ (Heyl 1990), a difference of up to 16 orders of magnitude.

These findings engaged our interest to elucidate chemical and physical effects upon Galactic cosmic-ray MeV ion interaction with frozen organic samples, resulting in the formation of new molecules in interstellar ices. Kaiser & Roessler (1997, hereafter Paper I) and Kaiser et al. (1997, hereafter Paper II) of this series disclosed precise mechanistic information on the synthesis of the most primitive atom and molecule, atomic and molecular hydrogen, as well as complex species such as polycyclic aromatic hydrocarbons

(PAHs). Our present investigations focus on methane, ethylene, and acetylene as model compounds to elucidate detailed mechanisms to form intermediate sized neutral hydrocarbons such as C$_2$H$_x$ ($x = 1, \ldots, 6$) and C$_3$H$_x$ ($x = 4$, 6, 8) before extending studies to astrophysically relevant interstellar ice mixtures. The choice of MeV particles in our experiments characterizes the flux distribution maximum of Galactic cosmic-ray particles peaking at about 8–15 MeV (see discussion in Paper I), whereas experimental doses represent equivalent irradiation by the interstellar cosmic-ray particle field of about $1 \times 10^9$ yr. These mechanisms are investigated by (1) variation of the energy transfer from the implanted ion to the CH$_4$ target, the so-called averaged linear energy transfer (LET), from $4.0 \pm 0.2$ keV $\mu$m$^{-1}$ (7.3 MeV protons) to $45 \pm 5$ keV $\mu$m$^{-1}$ (9 MeV $\alpha$-particles); (2) increasing the absorbed energy per target molecule, dose D, to 30 eV; (3) elucidating diffusion limited chemistry of atoms, CH, CH$_2$, as well as CH$_3$ radicals via substitution of CH$_4$ by CD$_4$; and (4) changing the carbon to hydrogen ratio from 4:1 (CH$_4$) via 2:1 (C$_2$H$_4$) to 1:1 (C$_2$H$_2$). Further, CH$_4$/CD$_4$ mixtures are irradiated to differ between inter- and intra-molecular reactions, while $^{13}$CH$_4$ targets are selected to verify on line and *in situ* Fourier transform infrared (FTIR) spectroscopy and quadrupole mass spectrometry (QMS) data.

## 2. EXPERIMENTAL APPROACH AND COMPUTATIONAL MODEL

The simulation experiments were performed in a UHV chamber equipped with a closed cycle helium refrigerator and an attached silver wafer (Kaiser, Gabrysch, & Roessler 1995). Ice layers are prepared by depositing gases on a cooled wafer, keeping the cold finger at 10 K for 60 minutes, heating the ices to 35 K with 0.005 K s$^{-1}$, equilibrating at 35 K for 1 hr, and cooling down to 10 K with 0.005 K s$^{-1}$. This temperature program ensures a well-defined low-temperature modification of all ices. Further, a constant LET is crucial to guarantee target-depth–invariant reaction mechanisms, and the target thickness must be limited to $5 \pm 1$ $\mu$m, well below the range of 7.3 MeV protons and 9 MeV $\alpha$-particles with about 930 and 130 $\mu$m. Hydrocarbon free UHV conditions of about $4 \times 10^{-10}$ mbar are supplied by a membrane, molecular drag, and cryopump proved to be essential to exclude organic contamination and restrict condensation of residual gases onto the silver waver to one monolayer in $\approx$ 10 hr. All targets are irradiated at 10 K with ion fluxes $\phi$ of 9.0 MeV $\alpha$-particles and 7.3 MeV protons adjusted to $\phi (\alpha) = 127$ nA cm$^{-2}$ and $\phi (p) = 111$ nA cm$^{-2}$ to limit the temperature increase of the frost surface to $14 \pm 1$ K. After the irradiation, all targets are warmed up to 293 K. Isotopically pure gases are supplied by MSD isotopes [$^{13}$CH$_4$ (99.9% $^{13}$C); CD$_4$ (99.9% D); $^{12}$CH$_4$ (99.9% $^{12}$C)] and are used without further purification.

The solid state is monitored on line and *in situ* with a Fourier transform infrared (FTIR) spectrometer (4000–400 cm$^1$, NICOLET) in absorption-reflection. Table 1 compiles those species and their absorption coefficients whose concentration profiles of which have been quantified via the Lambert-Beer relation (1):

$$I(\tilde{v}) = I_0(\tilde{v})e^{-\epsilon(\tilde{v})n} , \qquad (1)$$

with the intensity of the IR beam after, $I(\tilde{v})$, and before absorption, $I_0(\tilde{v})$, at a wavenumber $\tilde{v}$, the wavenumber-dependent absorption coefficient $\epsilon(\tilde{v})$ (in units of cm$^{-2}$) and

TABLE 1

INTEGRAL ABSORPTION COEFFICIENTS $A_{exp}$, INTEGRATION LIMITS, AND MODES OF QUANTIFIED SPECIES
DURING THE IRRADIATION EXPERIMENTS

| Species | Vibration | Integration limits (cm$^{-1}$) | $A_{exp}$ (cm) | Reference |
|---|---|---|---|---|
| $CH_3$ | $\nu_2$ | 629–590 | $(2.5 \pm 0.8) \times 10^{-17}$ | 1, 2 |
| $CH_4$ | $\nu_4$ | 1349–1249 | $(6.2 \pm 0.6) \times 10^{-18}$ | 3 |
| | $\nu_3 + \nu_4$ | 4483–4246 | $(3.5 \pm 0.5) \times 10^{-18}$ | 3 |
| | $\nu_1 + \nu_4$ | 4231–4168 | $(1.6 \pm 0.4) \times 10^{-18}$ | 3 |
| | $3\nu_4$ | 3860–3830 | $(2.0 \pm 0.3) \times 10^{-19}$ | 3 |
| | $\nu_2 + \nu_4$ | 2887–2784 | $(2.3 \pm 0.4) \times 10^{-18}$ | 3 |
| $C_2H_2$ | $\nu_3$ | 3269–3209 | $(3.2 \pm 0.3) \times 10^{-17}$ | 4 |
| | $\nu_4 + \nu_5$ | 1449–1359 | $(4.6 \pm 0.5) \times 10^{-18}$ | 4 |
| | $\nu_5$ | 809–729 | $(1.4 \pm 0.2) \times 10^{-17}$ | 4 |
| | $\nu_2$ | 1990–1960 | $(1.0 \pm 0.3) \times 10^{-19}$ | 4 |
| $C_2H_4$ | $\nu_{11}$ | 2987–2951 | $(1.0 \pm 0.2) \times 10^{-18}$ | 5 |
| | $\nu_7$ | 1023–837 | $(1.5 \pm 0.3) \times 10^{-17}$ | 5 |
| $C_2H_6$ | $\nu_6$ | 1374–1360 | $(6.0 \pm 0.6) \times 10^{-19}$ | 3 |
| | $\nu_9$ | 830–817 | $(1.9 \pm 0.2) \times 10^{-18}$ | 3 |
| | $\nu_8$ | 1480–1445 | $(2.7 \pm 0.3) \times 10^{-18}$ | 3 |
| $C_nH_{2n+2}(n = 4, 5, 6, 7)$ | $\nu_{as}(CH_3)$ | 2965–2949 | $(2 \pm 1) \times 10^{-17}$ | 3 |
| | $\nu_{as}(CH_2)$ | 2921–2923 | $(3.8 \pm 1.4) \times 10^{-17}$ | 6 |
| | $\nu_s(CH_2)$ | 2855–2845 | $(6 \pm 3) \times 10^{-18}$ | 6 |
| | $\nu_s(CH_3)$ | 2875–2865 | $(3.0 \pm 1.5) \times 10^{-18}$ | 6 |
| $CH_xD_y$ $(x + y = 4)$ | pro CH | | $(1.5 \pm 0.2) \times 10^{-18}$ | 6 |
| | pro CD | | $(1 \pm 0.3) \times 10^{-18}$ | 3 |
| $CH_3CD_3$ | $vas(CH_3)$ | 2980–2970 | $(1 \pm 0.2) \times 10^{-17}$ | 3 |
| | $vas(CD_3)$ | 2200–2400 | $(3.6 \pm 0.5) \times 10^{-18}$ | 7 |
| $CD_4$ | $\nu_3$ | 2345–2329 | $(7 \pm 2) \times 10^{-18}$ | 7 |
| | $\nu_1 + \nu_4$ | 3150–3070 | $(8 \pm 3) \times 10^{-20}$ | 8 |
| | $3\nu_4$ | 2935–2920 | $(6 \pm 2) \times 10^{-20}$ | 8 |
| | $\nu_3 + \nu_4$ | 3261–3220 | $(4 \pm 1) \times 10^{-19}$ | 8 |
| | $\nu_4$ | 1010–980 | $(4 \pm 1) \times 10^{-18}$ | 8 |
| $C_2D_2$ | $\nu_3$ | 2433–2368 | $(1.5 \pm 0.5) \times 10^{-17}$ | 8 |
| | $\nu_5$ | 548–539 | $(0.7 \pm 0.3) \times 10^{-17}$ | 8 |
| $C_2D_4$ | $\nu_7$ | 748–606 | $(0.8 \pm 0.2) \times 10^{-17}$ | 8 |
| $C_2D_6$ | $\nu_7$ | 2235–2226 | $(1.0 \pm 0.5) \times 10^{-17}$ | 5, 9 |
| | $\nu_5$ | 2087–2077 | $(2 \pm 1) \times 10^{-18}$ | 5, 9 |
| | $\nu_9$ | 605–583 | $(1 \pm 0.3) \times 10^{-18}$ | 5, 9 |

REFERENCES.—Snelson (1970); 2. Wormhould & McCurdy (1989); 3. Pearl et al. (1991); 4. Pearl 1994, private communication; 5. Cowieson et al. (1981); 6. Bellamy (1968); 7. Kondo & Saeki (1973); 8. Addepalli & Rao (1976); 9. Smit, van Straten, & Visser (1978); 9. Nyquist et al. (1952).

the number of absorbing species (per cm$^2$), $n$. Reformulating equation (1) with $A(\tilde{\nu}) \equiv \log [I_0(\tilde{\nu})/I(\tilde{\nu})]$ gives

$$A(\tilde{\nu}) = \epsilon(\tilde{\nu})n/\ln 10 . \tag{2}$$

Integrating from $\tilde{\nu}_1$ to $\tilde{\nu}_2$ yields

$$n = \frac{\int_{\tilde{\nu}_1}^{\tilde{\nu}_2} A(\tilde{\nu}) \, d\tilde{\nu}(\ln 10)}{A_{exp}} \times \frac{\cos 62.5}{2} , \tag{3}$$

with the integrated absorption $\int_{\tilde{\nu}_1}^{\tilde{\nu}_2} A(\tilde{\nu}) \, d\tilde{\nu}$ in cm$^{-1}$ and the integral absorption coefficient $A_{exp} = \int_{\tilde{\nu}_1}^{\tilde{\nu}_2} \epsilon(\tilde{\nu}) \, d\tilde{\nu}$ in cm. The factor cos 62.5 accounts for the angle between the surface normal of the (111) silver wafer and the IR beam, while a division by 2 corrects for the ingoing and outgoing IR beam. This procedure is accurate within $\pm 10\%$–20%.

The gas phase is probed through a calibrated quadrupole mass spectrometer (QMS). Data processing is performed via matrix interval algebra (Kaiser et al. 1995). Briefly, $m/e$ ratios are chosen to result in an inhomogeneous system of linear equations including the measured ion current (right-hand vector), partial pressures (unknown quantity), and calibration factors of fragments of individual gaseous species determined in separate experiments. Since all quantities are provided with experimental errors, matrix interval arithmetic, i.e., an IBM high-accuracy arithmetic subroutine defining experimental uncertainties as intervals, is incorporated in the computations to extract individual, calibrated components of gas mixtures.

Physical processes triggered by the ion implantation into a $CH_4$ target are simulated with the MARLOWE program (Robinson 1990) extended for quantum mechanical and relativistic treatments of our MeV ions (Paper I). This code calculates elastic and inelastic energy transfers from an impinging particle to the target atom(s) of the condensed hydrocarbon ices.

## 3. RESULTS

### 3.1. Computer Simulations

#### 3.1.1. Elastic Energy Transfer

The MARLOWE calculations show that implanted $\alpha$-particles and protons transfer less than 1% of the energy via elastic encounters to the $CH_4$ target. Our result is consistent with previous investigations depicting a larger fraction of inelastic versus elastic energy loss if the kinetic energy of the projectile in keV amu$^{-1}$ is larger than the projectile's mass in atomic mass units (Roessler 1991). This energy transfer engages high energetic C, as well as H atoms holding themselves kinetic energies up to 17 and 28 keV, respectively. Since these energies are still 3 orders of magnitude too large to form stable chemical bonds, the kinetic energy has to be

released even further to the solid methane target resulting in the generation of collision cascades (see § 1). Averaging over $10^4$ simulated cascades, we find total numbers of about 0.2/0.07 C (7.3 MeV $H^+$) and 3–4 H/1.2 C atoms (9.0 MeV $\alpha$) per impinging MeV particle in a 5 $\mu$m $CH_4$ target. An increasing hydrogen to carbon ratio from 1 ($C_2H_2$) via 2 ($C_2H_4$) as compared to 4 ($CH_4$) studied earlier results in an enhanced ratio of H knock-ons versus C knock-ons, i.e., [H knock-ons]$_{C2H2}$/[C knock-ons]$_{C2H2}$ = 2, [H knock-ons]$_{C2H4}$/[C knock-ons]$_{C2H4}$ = 3, and [H knock-ons]$_{CH4}$/[C knock-ons]$_{CH4}$ = 10.

### 3.1.2. Inelastic Energy Transfer

The inelastic energy transfer dominates the moderation of the MeV projectiles in the solid hydrocarbon targets and results in generation of excitons (electronic excitations in the solid state). Grigorev, Pshezhetskii, & Trakhtenberg (1985) determined the first $CH_4$ exciton level (triplet) to 5.4 eV, while the second exciton level (singlet) ranges at 10.9 eV. The singlet state can be stabilized through phonon interactions to the triplet state, transfer its excess energy to the surrounding matrix or decay to methyl radicals, $CH_3$, and H atoms (asterisk indicates electronically excited):

$$CH_4^* \rightarrow CH_3 + H \ . \tag{4}$$

Although no detailed exciton calculations on solid ethylene and acetylene have been performed yet, electronically excited $C_2H_2$ molecules very likely relax to $C_2H$ and H atoms, while $C_2H_4$ can fragment to $C_2H_3$ radicals and H:

$$[C_2H_2]^* \rightarrow C_2H + H \ , \tag{5}$$

$$[C_2H_4]^* \rightarrow C_2H_3 + H \ . \tag{6}$$
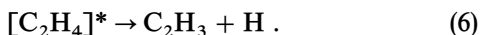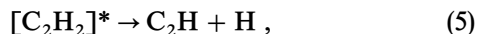
Besides formation of excitons, the inelastic energy transfer can ionize the target circa $10^{-16}$ to $10^{-15}$ s after the actual inelastic encounter (Moshammer 1990) if this process transfers more than the first ionization potential (12.7 eV) to the $CH_4$ molecule. This mechanism generates energetic electrons ($\delta$-electrons) released almost perpendicular to the MeV ion trajectory. Utilizing a model from Katz and coworkers to calculate the maximum range of these electrons (Katz et al. 1971), we calculate an upper limit of a 50 Å radius perpendicular to the trajectory of the implanted ion.
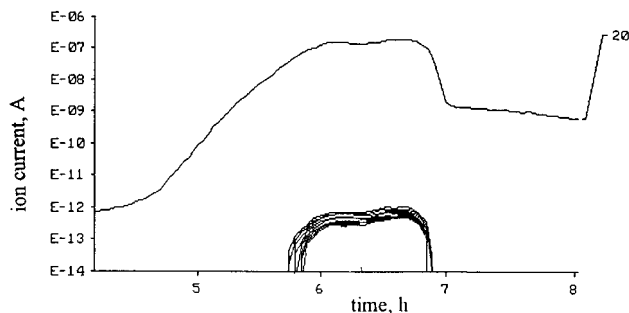
### 3.2. Quadrupole Mass Spectrometry (QMS)

#### 3.2.1. 10 K Irradiation

During the MeV particle irradiation of the methane targets only atomic as well as molecular hydrogen at $m/e = 1$ (H), 2 ($H_2$) ($CH_4$-target), 2 (D), 4 ($D_2$) ($CD_4$ target) and 1 (H), 2($D/H_2$), 3 (HD), and 4 ($D_2$) ($CD_4/CH_4$ target) could be detected. Their formation mechanisms are elucidated in Paper II. No sputtered $CH_x$ ($x = 1, \ldots, 4$) or higher masses were detected within the 1 amol detection limit of the mass spectrometer. During the irradiation phase of the $C_2H_2$ and $C_2H_4$ no atomic or molecular hydrogen was identified.

#### 3.2.2. Warming-up Phase to 293 K

Molecular ions of alkanes show pronounced maxima upon annealing the irradiated methane samples to 293 K (Fig. 1). At about 20 K, the sublimation of the remaining $CH_4/CD_4$ matrix releases matrix isolated alkane molecules up to $C_{11}D_{24}$. Correcting for the ionization cross section, we find [$CH_4$]/[alkane] ratios of about $10^3$–$10^4$. These patterns, however, do not go hand in hand with increasing molecular weights of sublimating products as expected from sublimation temperatures increasing by 14–16 K per additional $CH_2$ or $CD_2$ unit in alkanes. Here the sublimation sequence is reversed: $m/e = 180$ ($C_{11}D_{24}$) is detected first, while perdeutero propane $C_3D_8$ is monitored last. During the warm-up phase, the outer layers of the target, which were heated during the irradiation up to 15 K, are subliming prior to those layers close to the silver target, holding the 10 K temperature even during the actual irradiation. These findings strongly indicate that $C_{11}D_{24}$ is synthesized in target layers directly exposed to the ion beam, but that $C_3D_8$ is synthesized in target regions close to the Ag-(111) wafer. Hence, the increasing molecular weight of alkanes coincides with production zones of higher temperatures and infers a temperature-dependent component to their formation mechanism.

Besides a qualitative identification of alkanes up to $C_{14}H_{30}$ (9 MeV $\alpha$-particle irradiation) and $C_8H_{18}$ (proton experiments), data analyses via matrix algebra reveals production of unsaturated $C_3$-species methylacetylene, $CH_3CCH$, allene, $H_2CCCH_2$, propylene and cyclopropane, both $C_3H_6$ isomers, and $^{13}C$ substituted counterparts upon heating the irradiated target to 293 K (Table 2). Most strik-



FIG. 1a
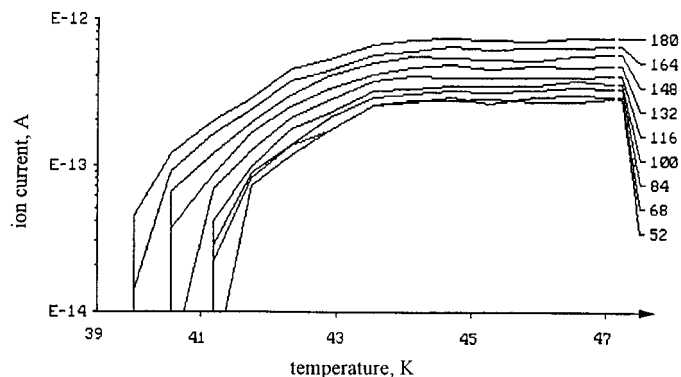
FIG. 1b

FIG. 1.—Detected alkanes during matrix sublimation of $CD_4$ ($m/e = 20$) after irradiation at 10 K at dose D = 30 eV; $m/e$-52, 58, 84, 100, 116, 132, 148, 164, and 180 (per-deutero propane → per-deutero undecane) define molecular ions. (a) Survey, (b) magnification of $m/e > 20$. The x-axis has been converted from time to temperature scale.

TABLE 2

HYDROCARBONS DETECTED IN THE WARM-UP PHASE OF IRRADIATED $CH_4$, $C_2H_4$, AND $C_2H_2$ TARGETS[a]

| Target | Hydrocarbons |
|---|---|
| Alkanes............................ | $CH_4$, $C_2H_6$, $C_3H_8$, $n-C_4H_{10}$, $i-C_4H_{10}$, $C_5H_{12}$ (dimethylpropane), $n/i - C_5H_{12}$, $C_6H_{14}$, $C_7H_{16}$, $C_8H_{18}$, $(C_9H_{20})$, $(C_{10}H_{22})$, $(C_{11}H_{24})$, $[(C_{12}H_{26})]$, $[(C_{13}H_{28})]$, $[(C_{14}H_{30})]$ |
| Unsaturated hydrocarbons...... | $C_2H_2$, $C_2H_4$, $C_3H_4$ (allene, methylacetylene), $C_3H_6$ (cyclopropane, propene) |

[a] Molecules in parentheses were not detected in proton-irradiated methane targets, and those in brackets were not in irradiated acetylene targets.

ing, $C_9H_{20}$, $C_{10}H_{22}$, $C_{11}H_{24}$, $C_{12}H_{26}$, $C_{13}H_{28}$, $C_{14}H_{30}$ were not synthesized in proton-irradiated methane targets, most likely due to a LET in this system 1 order of magnitude less as compared to $\alpha$-particle–irradiated methane samples. Since financial limitations restricted calibration of the deuterated molecules to $D_2$, $CD_4$, and $C_2D_x$ ($x = 2, 4, 6$), no information on $C_3D_x$ products was available.

### 3.3. *Fourier Transform Infrared Spectroscopy (FTIR)*

The FTIR spectra are analyzed in three steps. First, we investigate the absorptions qualitatively and assign their carriers. Hereafter the temporal developments upon MeV ion implantation of molecules and radicals with one and two carbon atoms are investigated quantitatively as outlined in § 2. Finally, these data are employed to calculate production rates $k(i, j)$ in units of synthesized molecules $i$ per MeV projectile $j$ in the solid target at 10 K. To calculate destruction rates per unit length, numbers given in the following section must be divided by the sample thickness, i.e., $4.0 \pm 0.4$ $\mu$m ($CH_4$ targets), $5.5 \pm 1.5$ $\mu$m ($CD_4$ targets), $2.5 \pm 0.3$ $\mu$m ($C_2H_4$ targets), and $3.0 \pm 0.1$ $\mu$m ($C_2H_2$ targets). The error bars of the destruction/formation rates are based on the fluctuating ion beam intensity ($\pm 10\%$–$20\%$) and the infrared integral absorption coefficients ($\pm 10\%$–$30\%$), see Table 1.

#### 3.3.1. *Qualitative Analyses*

##### 3.3.1.1 $^{12}CH_4$ and $^{13}CH_4$ Targets

The effects of the 7.3 MeV proton irradiation of the $^{12}CH_4$ target are displayed in Figure 2. A comparison of the pristine sample (Table 3) with the irradiated ice clearly shows absorptions of acetylene ($C_2H_2$), ethylene ($C_2H_4$), and ethane ($C_2H_6$) the features of which are compiled in Table 4. Open shell species, vinyl ($C_2H_3$, 898 cm$^{-1}$), ethyl ($C_2H_5$, 534 cm$^{-1}$), carbene ($CH_2$, 609 cm$^{-1}$), and methyl radicals ($CH_3$, 609 cm$^{-1}$) are present as well. Further, aliphatic absorptions of symmetric and asymmetric stretching vibrations of methyl ($CH_3$) and methylene ($CH_2$) groups can be assigned. The position of skeleton vibrations of alkanes infers predominantly branched hydrocarbons since absorption patterns for the $(CH_2)_n$ chain unit are only detected for $n = 1, 2, 3$, i.e., ethane $C_2H_6$, propane, $C_3H_8$, and $n$-butane, $C_4H_{10}$. Likewise, the fine structure of the symmetric deformation mode of the $CH_3$ group strongly supports the existence of tertiary butyl groups, $-C(CH_3)_3$. Further, substituted cycloalkanes such as cyclobutanes, pentanes, as well as hexanes are detected based on their skeleton vibrations. Besides aliphatic absorptions, olefinic groups are identified through their $=CH_2$ stretching vibrations, while mono- and disubstituted acetylene derivatives are assigned via C—H and C≡C stretching modes. Bombardments of $\alpha$-particles show qualitatively identical absorption patterns. The FTIR spectra of 9 MeV $\alpha$-particle–irradiated $^{13}CH_4$ targets underline these assignments and depict absorption patterns of similar per-$^{13}$C-substituted groups (Fig. 3, Tables 5 and 6).

##### 3.3.1.2. $CD_4$ Targets

In analogy to $^{12}CH_4$– and $^{13}CH_4$–irradiated targets, $CD_4$ samples show per-deutero ethane, ethylene, acetylene,
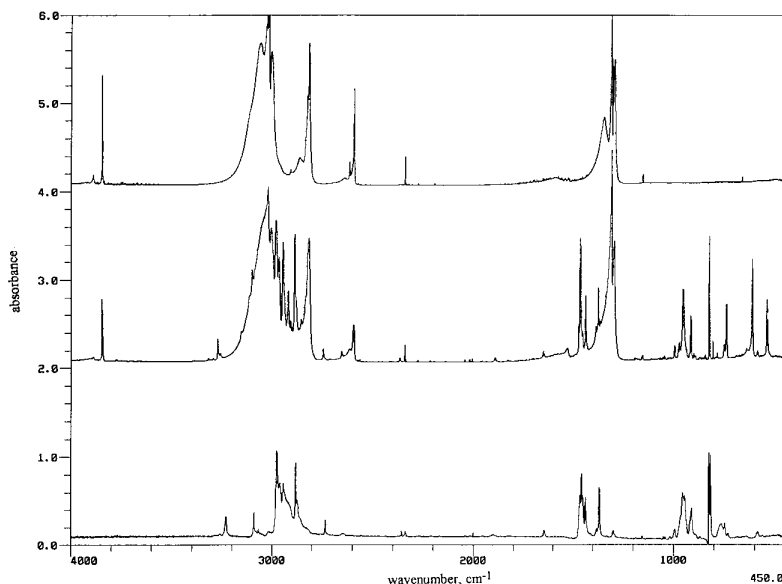


FIG. 2.—FTIR spectra of the $^{12}CH_4$ target before (*top*) and after (*middle*) a 7.3 proton irradiation at 10 K. Bottom spectrum was recorded at 60 K after sublimation of $CH_4$ and $C_2H_x$ ($x = 1, \ldots, 6$). Absorptions and assignments are compiled in Tables 3 and 4.

TABLE 3

FUNDAMENTAL AND COMBINATION BANDS OF SOLID $^{12}CH_4$ AT 10 K

| Vibration | Wavenumber (cm$^{-1}$) |
|---|---|
| $v_3 + v_4$ ....... | 4349, 4324, 4328, 4314.2, 4302.5, 4299.5, 4307.8, 4283.3 |
| $v_2 + v_3$ ....... | 4527.1, 4537 |
| $v_1 + v_4$ ....... | 4201.2, 4203.5, 4206.2 |
| $v_2 + 2v_4$ ...... | 4113.7, 4120.6 |
| $3v_4$ ........... | 3890.6, 3847.6, 3851.8, 3843.1 |
| $v_3$ ............ | 3114.5, 306.4, 3028, 3023.3, 3019.5, 3014.5, 3003, 3000 |
| $v_2 + v_4$ ....... | 2864.6, 2831, 2824.8, 2816.7, 2815.4, 2805.7 |
| $2v_4$ ........... | 2642, 2614.3, 2599.1, 2594.4, 2591.9 |
| $v_4$ ............ | 1596.1, 1350.7, 1309.2, 1303.5, 1298.6, 1295.5, 1293.6, 1290 |

TABLE 4

SELECTED ABSORPTIONS OF 7.3 MeV PROTON–IRRADIATED $^{12}CH_4$ AT 10 K[a]

| Assignment | Carrier and Wavenumber (cm$^{-1}$) |
|---|---|
| H—C≡C—R ................... | $v_{CH(sp)}$(3278, 3230, 3293, 3258), $v_{C≡C}$(2136, 2134) |
| RHC=C=CHR′ .............. | $v_{C=C=C}$(1934) |
| CH$_2$=C=CRR′ .............. | $v_{C=C=C}$(1923, 1918) |
| CH$_2$=C=CHR′ .............. | $v_{C=C=C}$(1943) |
| =CH$_2$($sp^2$) .................. | $v_{CH}$(3098), $v_{C=C}$(1643, 1650), $\delta_{ip}$(1417, 1419), $\delta_{op}$(890, 897) |
| —CH$_3$ ........................ | $v_{as}$(2964, 2962, 2958, 2954), $v_s$(2884), $\delta_b$(1472), $\delta_{as}$ (1457 1453, 1448), $\delta_s$ (1386, 1366) |
| —C(CH$_3$)$_2$— ................... | $\delta_s$(1386, 1366), $v_2$(1172), $v_3$(1157), $v_4$(842) |
| —CH$_2$— ($sp^3$) ................. | $v_{as}$(2958, 2934, 2917), $v_s$(2853), $\delta_b$(1457) |
| —(CH$_2$)$_n$—CH$_3$ ($n = 1, 2$) ...... | rocking (782, $n = 1$; 743, 749, $n = 2$) |
| —CH—($sp^3$) ................... | $v$(2898) |
| Substituted Cycloalkanes ...... | Skelet vibrations [$n = 6$: 1026, 1007, 993, 975, 970, 898(?)]; |
| C$_n$H$_{2n}$[$n = 6, 5, 4, 3$(?)] ........ | $n = 5$: 939, 935, 898 (?), 891 (?); $n = 4$: 926, 807; n = 3: 817 (?) |
| R—C≡C—R′ ................... | $v_{C≡C}$(2167, 2214, 2227, 2239, 2248) |
| Mono, o, m, p, 1.2.4-, .......... | Ring vibrations: 1607, 1593, 1581, $\delta_{op}$(870, 867: 1 free H; 855, |
| 1.3.5-substituted | 842: 2 free H), $\delta_{ip}$(1110, 1086, 1073, 1066, 1053, 1044, 1039, |
| Benzenes | 1026, 1039, 1026, 993, 975, 970: p and 1.2.4. substituted) |
| =CH$_2$($sp^2$) .................. | $v_{CH}$(3090, 3081.7, 3067) |
| =CH($sp^2$) ...................... | $v_{CH}$(3019) |

[a] R and R′ indicate organic groups.
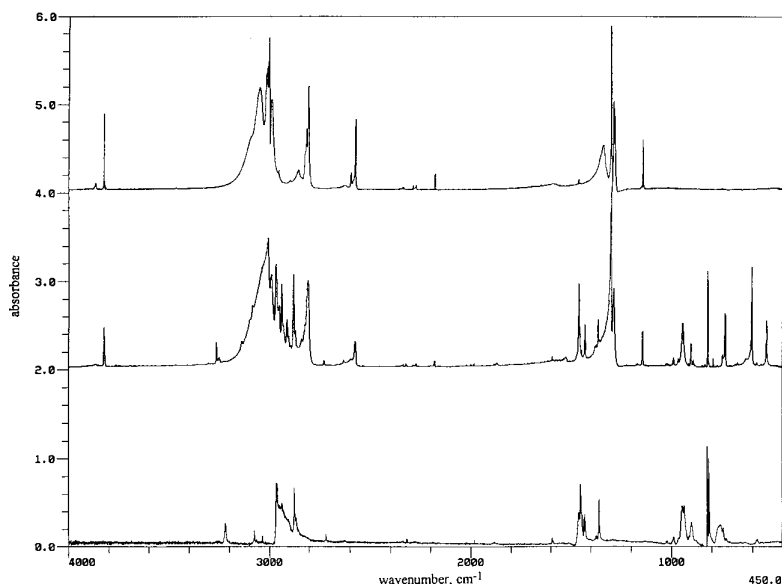


FIG. 3.—FTIR spectra of the $^{13}CH_4$ target before (top) and after (middle) a 9 MeV α-particle irradiation at 10 K. Bottom spectrum was recorded at 60 K after sublimation of $^{13}CH_4$ and $^{13}C_2H_x$ ($x = 1, ..., 6$). Absorptions and assignments are compiled in Tables 5 and 6.

TABLE 5

SELECTED ABSORPTIONS OF SOLID
$^{13}CH_4$ AT 10 K

| Vibration | Wavenumber (cm$^{-1}$) |
|---|---|
| $\nu_3 + \nu_4$ ........... | 4283 |
| $\nu_1 + \nu_3$ ........... | 4193 |
| $3\nu_4$ ............... | 3825 |

as well as methyl, vinyl, and ethyl radicals after the ion bombardment (Fig. 4, Tables 7 and 8). In strong contrast to § 3.3.1.1, however, aliphatic methyl and methylene absorptions show less pronounced absorption features. This finding correlates strongly with our QMS data: only perdeutero alkanes up to $C_{11}D_{24}$ could be probed in the deuterated samples, while hydrocarbons up to $C_{14}H_{30}$ were sampled in the $CH_4$ system.

### 3.3.1.3. $^{12}CH_4/CD_4$ Targets

Isotopically mixed species are prominent tracers for recombination and H-D-exchange reactions at 10 K (Paper II). FTIR spectra depict absorption of $CH_2D$ (563 cm$^{-1}$), $CHD_2$ (513 cm$^{-1}$), and $CHD_3$ (998.2 cm$^{-1}$; 1284.7 cm$^{-1}$) with rising dose. Most important, the mobility of $CH_2$, $CD_2$, $CH_3$, and $CD_3$ radicals starts between 60 and 75 K, well below our upper temperature limit of 15 K on the target surface. In strong coincidence, no scrambled recombination products $C_2H_2D_2$ ($CH_2 + CD_2$) and $C_2H_3D_3$ ($CH_3 + CD_3$) were detected, indicating that even reactions of neighboring carbon-containing hydrocarbon radicals are not detectable.

### 3.3.1.4. $C_2H_4$ Targets

The FTIR spectra of the irradiated $C_2H_4$ target are displayed in Figure 5 and shows modes of ethane, $C_2H_6$, [$v_9$ (822 cm$^{-1}$), $v_8$ (1464 cm$^{-1}$), $v_6$ (1374 cm$^{-1}$)], acetylene molecules, $C_2H_2$, [$v_1$ (3389 cm$^{-1}$), $v_3$ (3271 cm$^{-1}$), $v_5$ (736

TABLE 6

FTIR ABSORPTIONS OF 9 MeV $\alpha$-PARTICLE–IRRADIATED $^{13}CH_4$ AT 10 K

| Assignment | Carrier and Wavenumber (cm$^{-1}$) |
|---|---|
| H—$^{13}C\equiv^{13}C$—R ................ | $\nu_{CH(sp)}$(3264, 3251, 3248, 3220) |
| =$^{13}CH_2(sp^2)$ .................... | $\nu_{CH}$(3084, 3077, 3035), $\nu_{C=C}$(1643, 1650), $\delta_{ip}$(1417, 1419), $\delta_{op}$(890, 897) |
| —$^{13}CH_3$ ........................ | $\nu_{as}$(2969, 2962, 2958), $\nu_s$(2880), $\delta_{as}$(1464, 1454), $\delta_s$(1361, 1360) |
| —$^{13}C(^{13}CH_3)_2$— ................ | $\delta_s$(1386, 1366), $\nu_3$(1135), $\nu_4$(824, 820, 816) |
| —$^{13}CH_2$—$(sp^3)$.................. | $\nu_{as}$(2951, 2930), $\delta_b$(1433) |
| —$(^{13}CH_2)_n$—$^{13}CH_3$ $n = 1, 2$...... | rocking (764 $n = 1$; 745, $n = 2$) |
| —$^{13}CH$—$(sp^3)$ .................. | $\nu$(2880) |
| $^{13}R$—$^{13}C\equiv^{13}C$—$^{13}R'$ ............ | $\nu_{C\equiv C}$(2156, 2177, 2087, 2201) |
| Substituted benzenes .............. | 1030, 1028, 1026, 835, 793 |
| $^{13}CH_2$(carbene).................... | $\nu_2$(1108) |
| $^{13}CH_3$ radical ..................... | $\nu_2$(604) |
| $^{13}C_2H_5$ radical ................... | $\nu_9$(531) |
| $^{13}C_2H_3$ radical ................... | $\nu_7$(892) |
| $^{13}C_2H_2$ ........................... | $\nu_3$(3261), $\nu_5$(735) |
| $^{13}C_2H_4$ ........................... | $\nu_7$(956) |
| $^{13}C_2H_6$ ........................... | $\nu_8$(1460), $\nu_6$(1366), $\nu_9$(820) |
| =$^{13}CH_2(sp^2)$ .................... | $\nu_{CH}$(3076) |
| =$^{13}CH(sp^2)$ ..................... | $\nu_{CH}$(3034) |
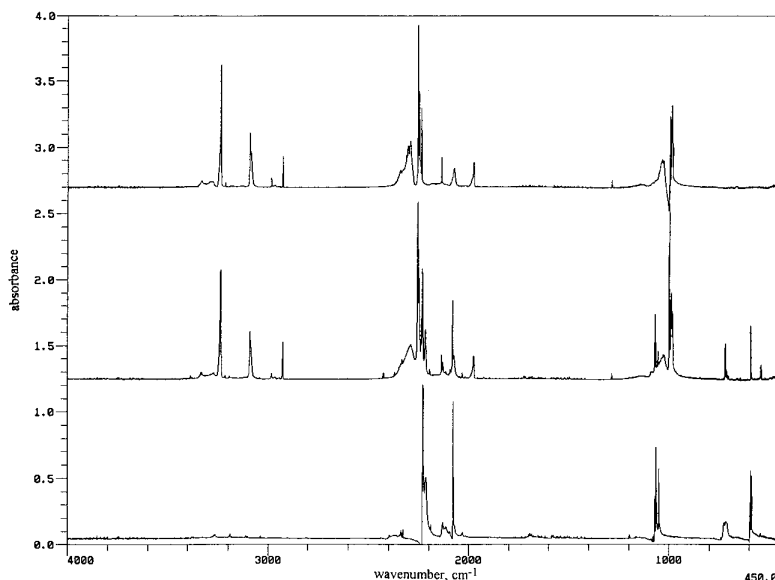


FIG. 4.—FTIR spectra of the $CD_4$ target before (*top*) and after (*middle*) a 9 MeV $\alpha$-particle irradiation at 10 K. Bottom spectrum was recorded at 60 K after sublimation of $CD_4$ and $C_2D_x$ ($x = 1, \ldots, 6$). Absorptions and assignments are compiled in Tables 7 and 8.

TABLE 7

SELECTED ABSORPTIONS OF SOLID $CD_4$ AT 10 K

| Vibration | Wavenumber (cm$^{-1}$) |
|---|---|
| $2\nu_3$............ | 4479.5, 4477, 4505 |
| $\nu_3 + 2\nu_4$...... | $4222(+\nu_1)$, $4217.9(+\nu_1)$, 4195 |
| $\nu_3 + \nu_4$....... | 3236, 3277 $(+\upsilon_L)$, 3287$(+\upsilon_L)$ |
| $\nu_1 + \nu_4$....... | 3092.2, 3086.6 |
| $3\nu_4$............ | 2930, 2926.7, 2925 |
| $\nu_3$............ | 2255, 2249, 2238, 2232, 2217.8, $2290(+\upsilon_L)$ |
| $2\nu_4$............ | 1975, 1973.6, $2002(+\upsilon_L)$ |
| $\nu_4$............. | 1000, 998, 996, 993, 989.6, 987.6, 985, 982 |

TABLE 8

FTIR ABSORPTIONS OF 9 MeV α-PARTICLE–IRRADIATED $CD_4$ AT 10 K

| Assignment | Carrier and Wavenumber (cm$^{-1}$) |
|---|---|
| $D-C\equiv C-R$ ...... | $\nu_{CD(sp)}$(2395, 2336, 2348, 2340), |
| $-CD_3$............ | $\nu_{as}$(2218), $\delta$(1062) |
| $-CD_2-(sp^3)$...... | $\nu_{as}$(2116), $\nu_s$(2032, 2028, 2017) |
| $C_2D_6$............ | $\nu_7$(2232), $\nu_5$(2081) |
| $C_2D_4$............ | $\nu_7$(722), $\nu_{12}$(1069) |
| $C_2D_2$............ | $\nu_3$(2427), $\nu_5$(543) |
| $C_2D_3$............ | $\nu_7$(705) |
| $C_2D_5$............ | $\nu_1$(2197), $\nu_3$(2046) |
| $CD_3$............ | $\nu_2$(460), $\nu_3$(2372), $\nu_4$(1024) |
| $C_2D_2$............ | $\nu_2$(847) |

cm$^{-1}$)], as well as ethyl radicals, $C_2H_5$, [$\upsilon_9$ (542 cm$^{-1}$)]. $C_2H_3$ radicals as detected in irradiated $CH_4$ targets could not be sampled. This finding is consistent with previous matrix isolation studies, showing that $C_2H_3$ is only stable in noble gas and methane matrices. As the radiation dose increases, acetylenic, olefinic, and even aliphatic structures were probed (see Tables 9 and 10).

### 3.3.1.5 $C_2H_2$ Targets

In strong contrast to $C_2H_4$ and $CH_4$ irradiation experiments, C—H stretching vibrations of monosubstituted

TABLE 9

SELECTED ABSORPTIONS OF SOLID $C_2H_4$ AT 10 K

| Vibration | Wavenumber (cm$^{-1}$) |
|---|---|
| $\nu_9$.................. | 3113 |
| $\nu_2 + \nu_{12}$........... | 3073 |
| $\nu_{12}$.................. | 1438 |
| $\nu_7$.................. | 951 |

TABLE 10

FTIR ABSORPTIONS OF 9 MeV α-PARTICLE–IRRADIATED $C_2H_4$ AT 10 K

| Assignment | Carrier and Wavenumber (cm$^{-1}$) |
|---|---|
| $H-C\equiv C-R$ ...... | $\nu_{CH(sp)}$(3231) |
| $=CH_2(sp^2)$........ | $\nu_{CH}$(3085, 3073), $\nu_{C=C}$(1642, 1647), $\delta_{ip}$(1419) $\delta_{op}$(893) |
| $-CH_3$.............. | $\nu_{as}$(2963), $\nu_s$(2871), $\delta_b$(1472), $\delta_{as}$(1457), $\delta_s$(1375) |
| $-CH_2-(sp^3)$...... | $\nu_{as}$(2928), $\nu_s$(2852) |
| $-CH-(sp^3)$....... | $\nu$(2898) |
| $R-C\equiv C-R'$...... | $\nu_{C\equiv C}$(2167, 2214, 2227, 2239, 2248) |
| $=CH_2(sp^2)$........ | $\nu_{CH}$(3240) |

TABLE 11

SELECTED ABSORPTIONS OF SOLID $C_2H_2$ AT 10 K

| Vibration | Wavenumber (cm$^{-1}$) |
|---|---|
| $\nu_1$.................. | 3373 |
| $\nu_3$.................. | 3270/3272 |
| $\nu_2$.................. | 1963 |
| $\nu_4 + \nu_5$............ | 1331 |
| $\nu_5$.................. | 736 |
| $\nu_4$.................. | 631 |
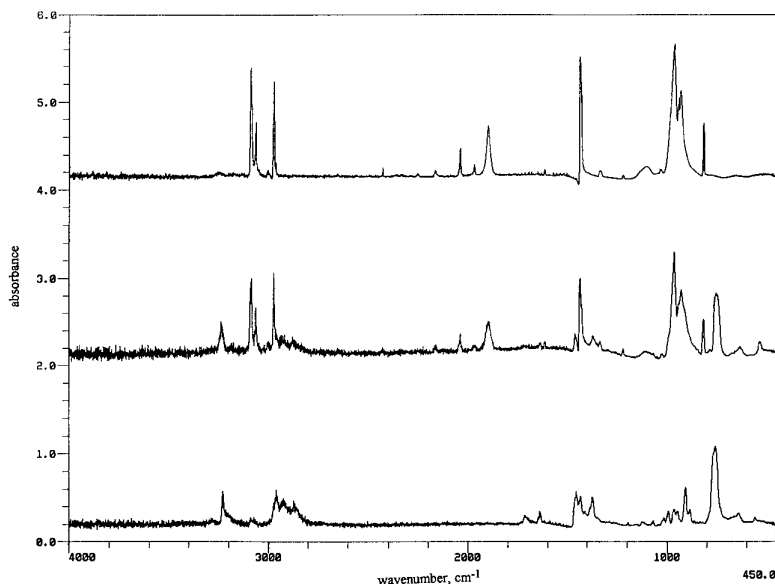


FIG. 5.—FTIR spectra of the $C_2H_4$ target before (*top*) and after (*middle*) a 9 MeV α-particle irradiation at 10 K. Bottom spectrum was recorded at 75 K after sublimation of the remaining $C_2H_4$. Absorptions and assignments are compiled in Tables 9 and 10.
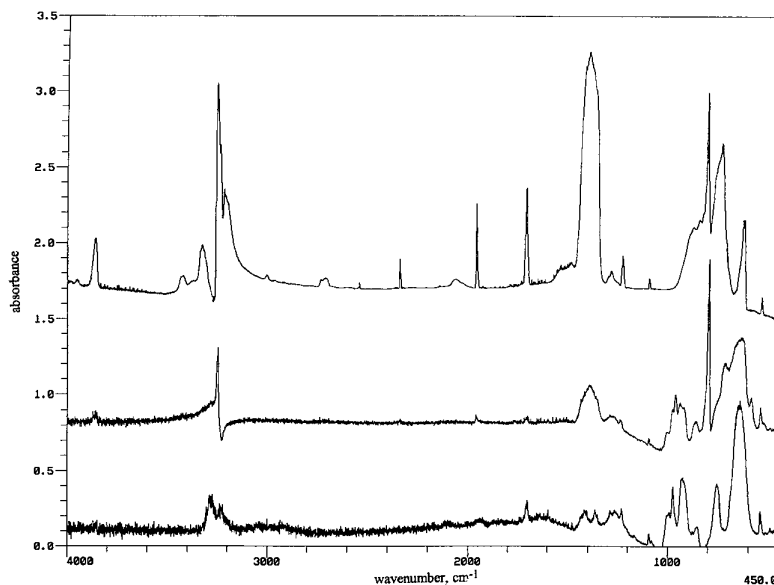
FIG. 6.—FTIR spectra of the $C_2H_2$ target before (*top*) and after (*middle*) a 9 MeV $\alpha$-particle irradiation at 10 K. Bottom spectrum was recorded at 75 K after sublimation of the remaining $C_2H_2$. Absorptions and assignments are compiled in Tables 11 and 12.

acetylenic and olefinic species dominate the FTIR spectra (Fig. 6, Tables 11 and 12). As already established in QMS analysis, the reduced H:C ratio of 1 as compared to 2 in the ethylene target hinders formation of higher alkanes. Likewise, no hydrogen rich species $C_2H_6$ and $C_2H_5$ were probed except weak absorptions of $C_2H_4$.

### 3.3.2. Quantitative Analyses

Figures 7–11 compile the temporal development of integrated absorptions of selected $CH(D)_x$ ($x = 2$, 3, 4) and $C_2H(D)_x$ ($x = 2$, 3, 4, 5, 6) species during the irradiation at 10 K and consecutive equilibration period at 10 K. Hereafter all molecules/radicals containing two carbon atoms will be referred to as C2 *species*. Considering these graphs, we calculate the destruction rates of the $CH_4/CD_4$ molecules, as well as production rates of selected molecules/radicals during the early irradiation stage. $^{13}CH_4$-irradiated targets show the same temporal concentration profile within the error limits of 10%–20% as compared to the $^{12}CH_4$ system and hence are not included.

The response of the $CH_4$ and $CD_4$ systems upon the MeV particle bombardment is governed by the formation of methyl, $CH_3$, and carbene, $CH_2$, radicals as well as their deuterated counterparts as the result of a dominating electronic energy loss (see § 3.1.2), and secondary radiolysis of

methyl radicals to carbene and atomic hydrogen as shown previously (Paper II):

$$CH_3 \rightarrow CH_2 + H . \qquad (5)$$

In addition, synthesized closed shell molecules acetylene, $C_2H_2$, ethylene, $C_2H_4$, and ethane, $C_2H_6$, as well as ethyl ($C_2H_5$) and vinyl ($C_2H_3$) radicals and their perdeutero analogs contribute 86%–91% to all newly formed molecules containing at least two carbon atoms. Here the production rates (Tables 13–15) give valuable insights in the formation mechanism of these C2 species. As expected from a hydrogen-rich target (C:H = 1:4), fully saturated alkanes, in this case ethane, hold large production rates of C2 species with $670 \pm 270$ synthesized $C_2H_6$ molecules per 9 MeV $\alpha$-projectile into the $CH_4$ target followed by the olefine $C_2H_4$ ($280 \pm 150$) and the acetylenic C2 species

TABLE 12

FTIR ABSORPTIONS OF 9 MeV $\alpha$-PARTICLE–IRRADIATED $C_2H_2$ AT 10 K

| Assignment | Carrier and Wavenumber (cm$^{-1}$) |
|---|---|
| H—C≡C—R | $\nu_{CH}(sp)(3283)$, 3281, 3229, 3219), $\nu_{C≡C}(2137, 2116, 2110, 2087)$ $\delta_{H-C≡}(642)$ |
| CH$_2$=C=CRR′ | $\nu_{C=C=C}(1926, 1918)$ |
| =CH$_2$ | $\nu_{CH(sp2)}(3084)$, $\delta$ip(1407, 1418) |
| =CH(aromatic/sp$^2$) | $\nu_{CH}(3040$-30), $\nu_{C=C}(1643, 1650)$, $\delta_{ip}(1417, 1419)$, $\delta_{op}(890, 897)$ |
| di-, tri- and tetra-substituted benzenes | 1365, 1280, 1265, 1233, 1093, 1081, 1036, 1004, 997, 975, 929, 855,756 |
| CH$_2$=C=CHR′ | $\nu_{C=C=C}(1958)$ |
| CH, $sp^3$ (?) | 3000-2700; 2984, 2933, 2924 |

TABLE 13

PRODUCTION AND DESTRUCTION ($CH_4$) RATES OF SELECTED SPECIES DURING MeV ION BOMBARDMENT AT 10 K OF $\alpha/CH_4$, $p/CH_4$, AND $\alpha/CD_4$ SYSTEMS

| Target $j$/Species $i$ | $\alpha/CH_4$ | $p/CH_4$ | $\alpha/CD_4$ |
|---|---|---|---|
| $CH_4$ | $-1320 \pm 300$ | $-110 \pm 15$ | $-1040 \pm 310$ |
| $CH_3$ | $320 \pm 150$ | $37 \pm 15$ | $60 \pm 40$ |
| $C_2H_6$ | $670 \pm 270$ | $122 \pm 62$ | $160 \pm 110$ |
| $C_2H_4$ | $280 \pm 150$ | $32 \pm 13$ | $42 \pm 20$ |
| $C_2H_2$ | $87 \pm 60$ | $11 \pm 3$ | $13 \pm 10$ |

TABLE 14

RATIO OF PRODUCTION RATES OF C2-SPECIES CALCULATED FROM TABLE 13

| C2-Species | Ratio |
|---|---|
| $k(C_2H_6, \alpha/CH_4)/k(C_2H_6, p/CH_4)$ | $9 \pm 7$ |
| $k(C_2H^4, \alpha/CH_4)/k(C_2H_4, p/CH_4)$ | $12 \pm 10$ |
| $k(C_2H_2, \alpha/CH_4)/k(C_2H_2, p/CH_4)$ | $10 \pm 8$ |
| $k(C_2H_4, \alpha/CH_4)/k(C_2D_6, \alpha/CD_4)$ | $10 \pm 8$ |
| $k(C_2H_4, \alpha/CH_4)/k(C_2D_4, \alpha/CD_4)$ | $11 \pm 9$ |
| $k(C_2H_2, \alpha/CH_4)/k(C_2D_2, \alpha/CD_4)$ | $25 \pm 24$ |
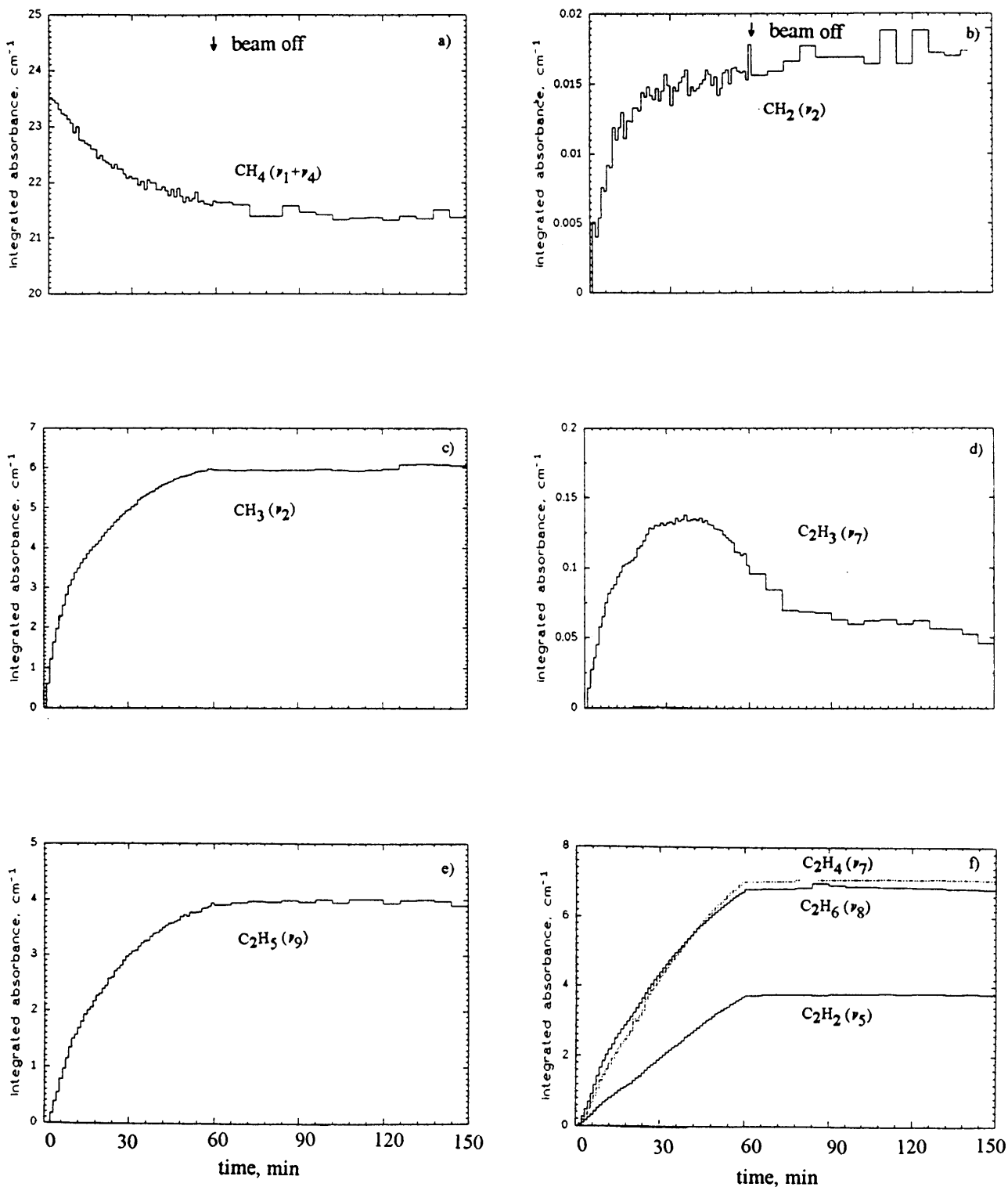
FIG. 7.—Temporal development of integrated absorptions of selected species in the $p/CH_4$ system: (a) $CH_4$ $(v_1 + v_4)$; (b) $CH_2$ $(v_2)$; (c) $CH_3$ $(v_2)$; (d) $C_2H_3$ $(v_7)$; (e) $C_2H_5$ $(v_9)$; (f) $C_2H_6$ $(v_8)$, $C_2H_4$ $(v_7)$, $C_2H_2$ $(v_5)$.

$C_2H_2$ (87 ± 60). Comparing these numbers with those in the $p/CH_4$ system, we find qualitatively the same trend, i.e., production rates of $C_2H_6 > C_2H_4 > C_2H_2$. However, the absolute production rates of ethane, ethylene, and acetylene are about a factor of 10 larger in the $\alpha/CH_4$ system than in the second one ($p/CH_4$). This order of magnitude correlates strongly with the ratio of the linear energy transfers (LET) of both systems, LET($\alpha/CH_4$)/LET($p/CH_4$) = 10 ± 1. Since

the MARLOWE calculations reveal a dominant inelastic energy loss, the formation mechanism of the C2 species is expected to be strongly correlated with this energy transfer process (see § 4). Finally, it is worth mentioning that the production rates of the C2 species in the $\alpha/CH_4$ system is larger by 1 order of magnitude as compared to irradiated $CD_4$ samples. This finding very likely points to an isotope effect in the formation of ethane, ethylene, and acetylene as
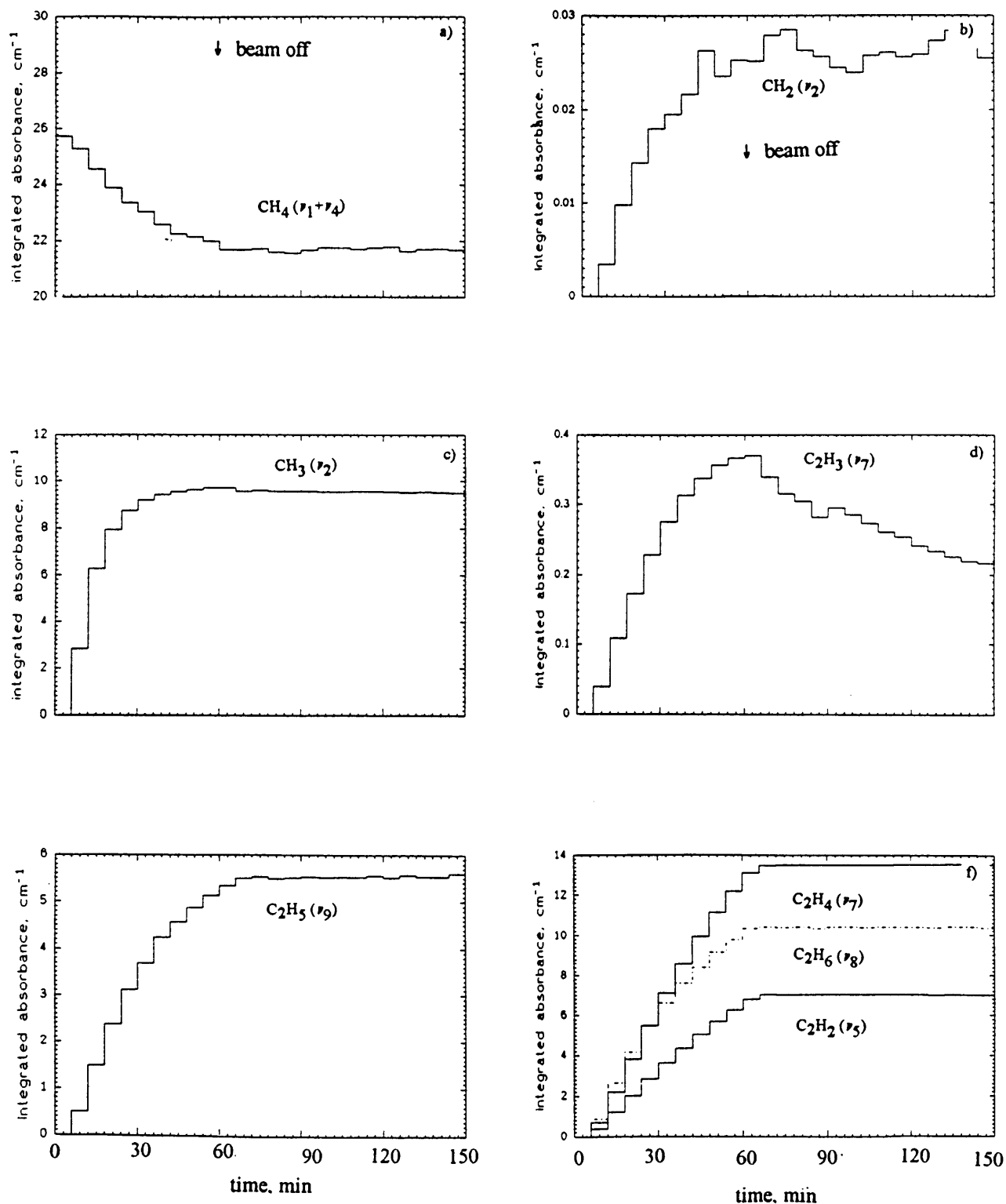
FIG. 8.—Temporal development of integrated absorptions of selected species in the $\alpha/CH_4$ system: (a) $CH_4$ $(v_1 + v_4)$; (b) $CH_2$ $(v_2)$; (c) $CH_3$ $(v_2)$; (d) $C_2H_3$ $(v_7)$; (e) $C_2H_5$ $(v_9)$; (f) $C_2H_6$ $(v_8)$, $C_2H_4$ $(v_7)$, $C_2H_2$ $(v_5)$.

already documented in an enhanced production of $H_2$ versus $D_2$ and $CH_3$ versus $CD_3$ in these targets.

Compared to the $\alpha/CH_4$ system, the production rates of $C_2H_6$ and $C_2H_2$ in hold the same magnitude within the experimental error limits in irradiated $C_2H_4$ targets, i.e., $240 \pm 130$ and $540 \pm 350$ $(\alpha/C_2H_4)$ versus $670 \pm 270$ and $87 \pm 60$ $(\alpha/CH_4)$.

A quantitative analysis of the $C_2H_2$ system reveals an enhanced destruction rate of the $C_2H_2$ molecules as compared to the $CH_4$ system, i.e., $4030 \pm 830$ and $1320 \pm 300$, and only a minor production rate of $3 \pm 2$ $C_2H_4$ molecules. This pattern correlates with formation of a solid residue upon annealing the $C_2H_2$ target to 293 K. Neither $CH_4$ nor $C_2H_2$ samples irradiated at identical doses, pressures,
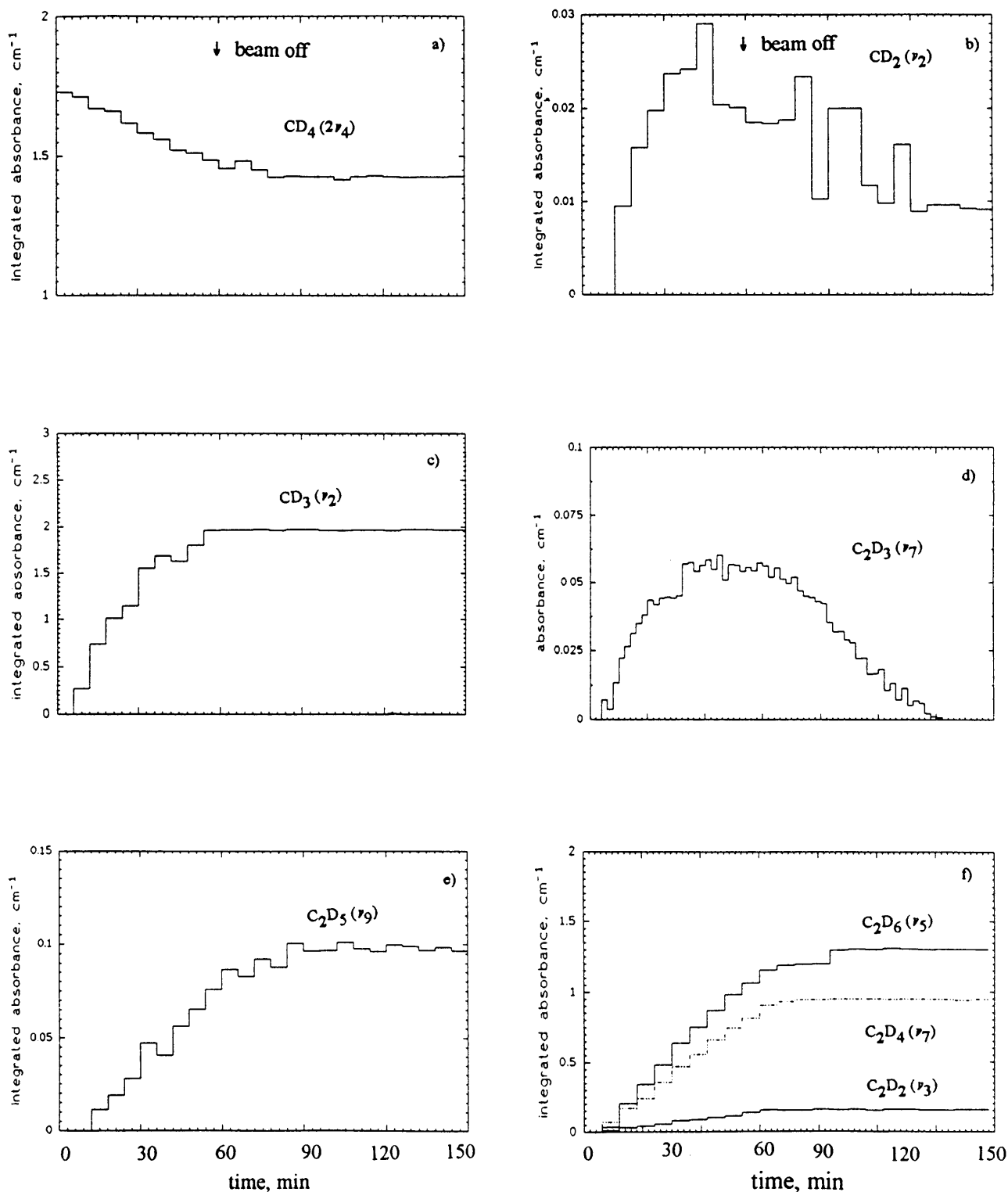
FIG. 9.—Temporal development of integrated absorptions of selected species in the $\alpha/CD_4$ system: (a) $CD_4$ ($2v_2$); (b) $CD_2$ ($v_2$); (c) $CD_3$ ($v_2$); (d) $C_2D_3$ ($v_7$); (e) $C_2D_5$ ($v_9$); (f) $C_2D_6$ ($v_5$), $C_2D_4$ ($v_7$), $C_2D_2$ ($v_3$).

LETs, and temperatures show these residues at room temperature (Paper I), indicating that a critical C:H ratio is essential to form these residues.

## 4. DISCUSSION

### 4.1. Formation of Molecules with one Carbon Atom

The synthesis of $CH_3$ and $CH_2$ radicals is strongly correlated to the formation of atomic and molecular hydrogen (Paper II). Since the LET in all systems is governed by inelastic energy transfers to the solid target, the exciton formation dominates followed by a decay to [$CH_3$ .... H] and [$CD_3$ .... D] radical pairs. This pair is matrix isolated by surrounding $CH_4$ molecules, and its fate determined by the remaining kinetic energy of the H/D atom. If the diffusion barrier can be passed, the radical pair separates to mobile H/D atoms but nonmobile $CH_3$ radicals. Otherwise,
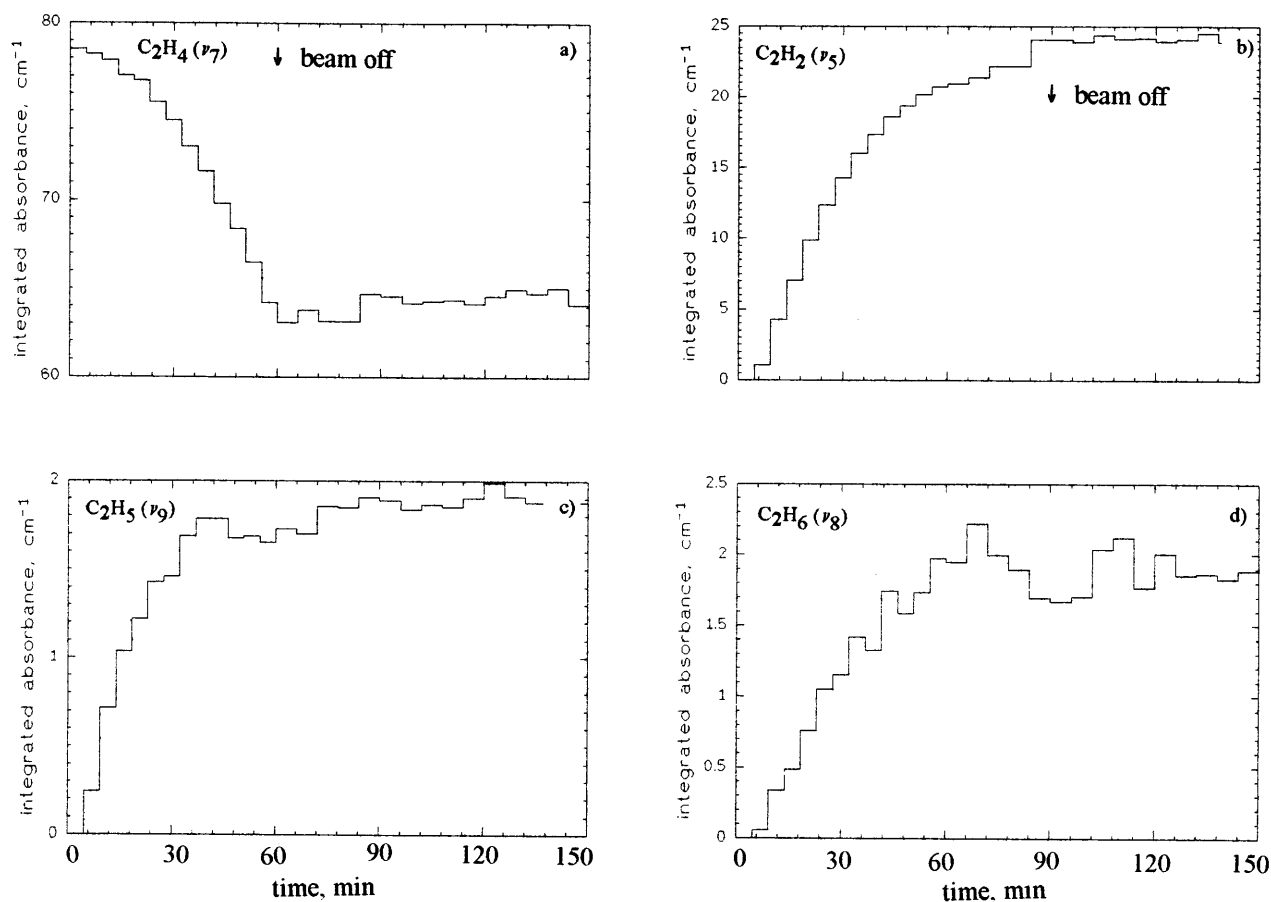
FIG. 10.—Temporal development of integrated absorptions of selected species in the $\alpha/C_2H_2$ system: (a) $C_2H_2$ ($v_2 + v_4$); (b) $C_2H_4$ ($v_{12}$)

a reverse reaction to $CH_4$ takes place. These processes are well documented by detection of HD as a recombination product of H and D atoms as well as probing $CHD_3$ molecules formed thru recombination of $CD_3$ and H atoms in $CH_4/CD_4$ targets at doses $D > 9$ eV. Likewise, the increased production rates of $CH_3$ versus $CD_3$ of $320 \pm 150$ and $60 \pm 40$, respectively, together with a higher $H_2$ yield as compared to $D_2$ underline the role of an enhanced H atom diffusion coefficient versus D atoms. Here the separation of the [$CH_3$ .... H] radical pair to methyl radicals and atomic hydrogen is facilitated owing to the lower mass of the H atom. To a minor amount, secondary dissociation of $CH_3$ forms H and $CH_2$.

### 4.2. Formation of Molecules with Two Carbon Atoms

#### 4.2.1. $C_2H_2$

Since the experiments were performed under bulk conditions, we cannot probe the spin state of the suprathermal

carbon atoms prior to reaction explicitly. The resonance rule, however, predicts that only carbon atoms in their $^3P_j$ and $^1D_2$ states are formed; potential carbon ions are neutralized before chemical forces take over (Stöcklin 1969, and references therein). The insertion of a carbon atom into the C—H bond of a single $CH_4$ molecule to internally excited methylcarbene [H—C—$CH_3$]* (reaction 1, Fig. 12), represents the primary reaction step in strong analogy to gasphase reactions studied (Stöcklin 1969; Dubrin, McKay, & Wolfgang 1964; McKay & Wolfgang 1961). C($^3P_j$) reacts to triplet methylcarbene, while C($^1D_2$) leads to the singlet counterpart. As expected from a short lifetime of less than 1 ps, no reactive methylcarbene intermediate could be sampled via FTIR spectroscopy. Methylcarbene undergoes $H_2$ elimination (singlet methylcarbene; reaction 2) or fragments to two H atoms (triplet carbene; reaction 3) to form an acetylene molecule. Here the key role of H atoms/$H_2$ molecules is well documented in terms of an isotope effect in an enhanced production rate of an $C_2H_2$ versus $C_2D_2$ of $25 \pm 24$. Since no isotopically scrambled HCCD was detected in $CH_4/CD_4$ irradiated samples, recombination of CH and CD to form acetylene can be clearly ruled out.

#### 4.2.2. $C_2H_4$

In the solid state, methylcarbene can transfer its excess energy to the surrounding matrix and thermalizes (reaction 4); alternatively, singlet methylcarbene can undergo [1, 2]-H-migration to form ethylene, reaction 5 which can be stabilized itself to form a thermal ethylene molecule, reaction 6. Previous isotope studies showed that a two-

TABLE 15

PRODUCTION AND DESTRUCTION RATES OF SELECTED SPECIES DURING
MeV ION BOMBARDMENT AT 10 K OF $\alpha/CH_4$, $\alpha/C_2H_4$, AND
$\alpha/C_2H_2$ SYSTEMS

| Target $j$/Species $i$ | $\alpha/CH_4$ | $\alpha/C_2H_4$ | $\alpha/C_2H_2$ |
|---|---|---|---|
| $CH_4$ .............. | $-1320 \pm 300$ | ... | ... |
| $C_2H_6$ .............. | $670 \pm 270$ | $240 \pm 130$ | $0$ |
| $C_2H_4$ .............. | $280 \pm 150$ | $-320 \pm 95$ | $3 \pm 2$ |
| $C_2H_2$ .............. | $87 \pm 60$ | $540 \pm 350$ | $-4030 \pm 830$ |
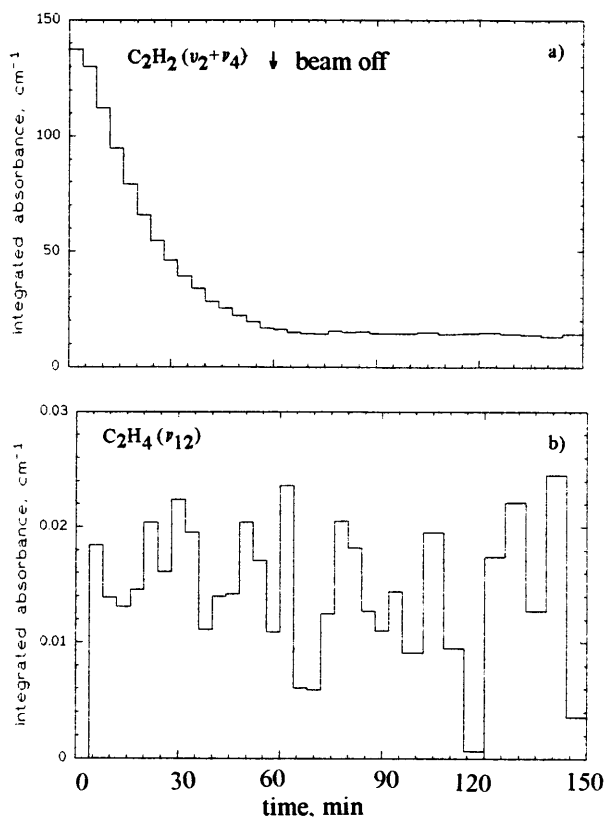
FIG. 11.—Temporal development of integrated absorptions of selected species in the $\alpha/C_2H_4$ system: (a) $C_2H_4$ ($v_7$); (b) $C_2H_2$ ($v_5$); (c) $C_2H_5$ ($v_9$); (d) $C_2H_6$ ($v_8$).

step process via C—H bond rupture in methylcarbene to H and vinyl radicals (reaction 7) followed by H atom addition can synthesize $C_2H_4$ as well (reaction 8; Taylor, Ache, & Wolf 1975). In addition, suprathermal CH radicals formed upon H atom abstraction by suprathermal carbon atom via reaction 9 can insert into a CH methane bond to build up a $C_2H_5$ radical (reaction 10). This intermediate

undergoes either C—H bond rupture to $C_2H_4$ via reaction 11 or thermalized to $C_2H_5$ radicals (reaction 12). The crucial role of the H atom in the formation of $C_2H_4$ is expressed in isotope effects as found in our experiments: the ratio of the ethylene production rates in $CH_4$ compared to $CD_4$ holds $11 \pm 9$ and can be explained in terms of a reduced rate constant in the rearrangement of methyl-carbene to ethylene (reaction 5) and/or through a hindered diffusion of D atoms versus H to form $C_2D_4/C_2H_4$ (reaction 8). Finally, we would like to point out that recombination of two $CH_2$ radicals to form an ethylene molecule does not contribute since no isotopically mixed $H_2CCD_2$ ($CH_2 + CD_2$) could be sampled. This finding strongly correlates to an onset of a $CH_2$ diffusion at 60 K as compared to our target temperature of 15 K.

### 4.2.3. $C_2H_6$

The synthesis of $C_2H_6$ can proceed through insertion of suprathermal carbene formed via reaction 13 into a C—H bond of a methane molecule followed by thermalization (reactions 14–15). An H atom addition to $C_2H_5$ can contribute to ethane as well (reaction 16). Here the isotopic effect expressed in the ratio of the production rates of $C_2H_6$ versus $C_2D_6$, i.e., $10 \pm 8$, strongly indicates a preferential H atom addition to $C_2H_5$ since the suprathermal pathway via $CH_2$ insertion is not expected to show an isotope effect. In strong coincidence with these results and §§ 4.2.1 and 4.2.2, no recombination radical-radical recombination could be sampled, here of two $CH_3$ radicals to $C_2H_6$. Again, the diffusion of $CH_3$ starts at about 70 K, much higher than our 14 K target.

The inability of the MeV particle irradiation of $C_2H_2$ to synthesize $C_2H_6$ molecules at 10 K and the extreme low production rate of $C_2H_4$ is well reflected in the C:H ratio of one in our sample. This trend is consistent with reduced production rates $k$ of $C_2H_6$ and $C_2H_4$ in irradiated, carbon-rich samples, i.e., $k(C_2H_6//\alpha/CH_4) > k(C_2H_6//\alpha/C_2H_4) > k(C_2H_6//\alpha/C_2H_2) = 670 \pm 270 > 240 \pm 130 > 0$ and $k(C_2H_4//\alpha/CH_4) > k(C_2H_4//\alpha)C_2H_2) = 280 \pm 150 > 3 \pm 2$.
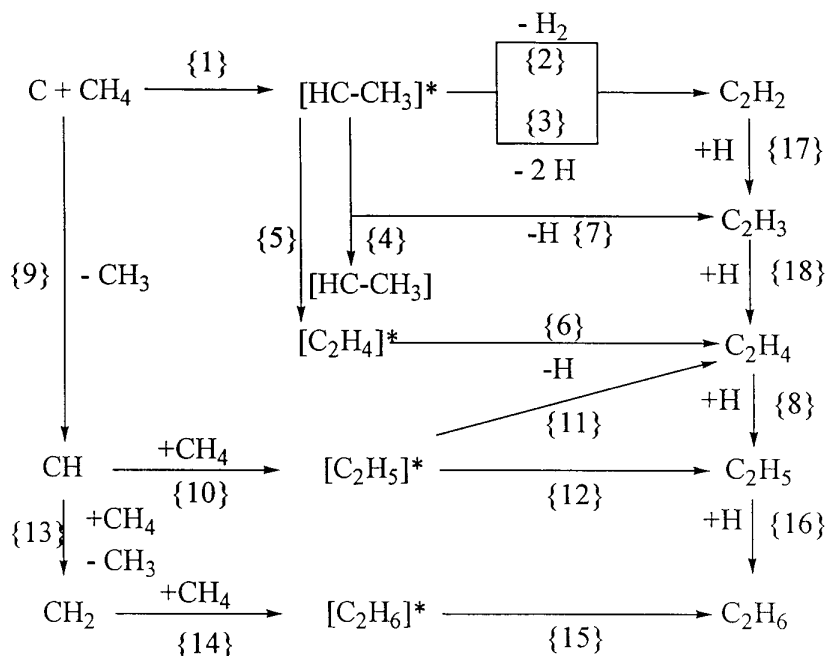


FIG. 12.—Compilation of mechanisms leading to formation of $C_2H_x$ species ($x = 2, 3, 4, 5, 6$)

Data analyses of the alkane distribution support this conclusion as well, and higher alkanes $C_{12}H_{26}$ to $C_{14}H_{30}$ were only synthesized in the $C_2H_4$ system.

### 4.2.4. $C_2H_3/C_2H_5$

Besides pathways already outlined in §§ 4.2.1–4.2.3, H atom addition to in situ synthesized $C_2H_2$ and $C_2H_4$ contributes to $C_2H_3$ (reaction 17) and $C_2H_5$ (reaction 8), respectively. These pathways have been confirmed in our experiments bombarding solid $C_2H_2$ and $C_2H_4$ at 10 K with 9 MeV $\alpha$-particles. Both reactions, however, hold entrance barriers of about 10.5 and 11.5 kJ mol$^{-1}$, respectively. Recalling that our target temperature is less than 15 K and that 100 kJ mol$^{-1}$ is equivalent to about 10,000 K, only suprathermal H/D atoms react via reactions 17 and 8.

### 4.3. Formation of Molecules with Three Carbon Atoms

The mechanism to form linear C3 species methylacetylene, $CH_3CCH$, allene, $H_2CCCH_2$, and propane, can be inferred from recent crossed molecular beam experiments of thermal atomic carbon $C(^3P_j)$ with $C_2H_4$ (Kaiser, Lee, & Suits 1996, and references therein). Here $C(^3P_j)$ reacts with $C_2H_4$ under addition to the $\pi$-bond to form a reactive cyclopropylidene intermediate (reaction 1 Fig. 13). This internally excited intermediate undergoes ring opening to allene (reaction 2). Since the crossed beam experiments were performed under single collision conditions, the allene intermediate cannot be stabilized in a third body reaction and fragments to atomic hydrogen and a propargyl radical, $C_3H_3$. In our solid state experiments, however, this excess energy of allene can be transferred to the surrounding $CH_4$ matrix, resulting in a "thermal" allene molecule, reaction 3. Further, H migration in allene to methylacetylene followed by thermalization could account for methylacetylene molecules, reaction 4. Since the energy of reactive C atoms in the present experiments is up to 20 times higher as compared to the crossed beam reactions, insertion in a single C—H bond of ethylene forming vinylcarbene (reaction 5) followed by H migration can contribute to allene (reaction 6) and/or methylacetylene (reaction 7) as well. Finally, the propane molecules are very likely formed through two successive H addition reactions to $C_3H_4$ intermediates or insertion of suprathermal $CH_2$. Again, we would like to point out that we neglect the discussion of different spin states and a potential role of intersystem crossing in the solid state since our MARLOWE calculations give no explicit information on the spin distribution.

### 4.4. Formation of Molecules with Four and More Carbon Atoms

Our FTIR data clearly indicate an onset of aliphatic —$CH_3$ and —$CH_2$ group absorption at doses as low as 0.1

eV, much smaller than the threshold dose to overlapping collision cascades. This finding strongly suggests that alkanes and cycloalkanes are formed inside a single collision cascade at lower doses and not through a successive insertion of thermal carbene, $CH_2$, into aliphatic C—H bonds like the reaction sequence

$$CH_2 + CH_4 \rightarrow CH_3-CH_3 \,, \qquad (6)$$

$$CH_3-CH_3 + CH_2 \rightarrow CH_3-CH_2-CH_3 \,, \qquad (7)$$

$$CH_3-CH_2-CH_3 + CH_2 \rightarrow i/n-C_4H_{10}, \text{ etc} . \qquad (8)$$
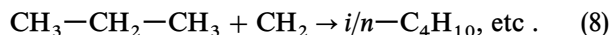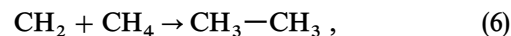
As shown in § 3, the alkane formation correlates with the temperature profile of the irradiated target, and per-deutero undecane, $C_{11}D_{24}$, is predominantly formed in target zones heated to 15 K, while lower alkanes such as per-deutero butanes, $C_4D_{10}$, are preferentially synthesized in cooler regions. Since the diffusion coefficient of the D atoms and $D_2$ molecules are enhanced by a factor of 3–5 in the 15 K regions as compared to 10 K zones, an increasing D recombination to $D_2$ and a diffusion to the vacuum-$CD_4$ surface boundary followed by a $D_2$ release into the gas-phase results in a carbon enrichment in these outer 15 K layers. Therefore, a multicenter reaction mechanism, similar to the formation of polycyclic aromatic hydrocarbons (PAHs; Paper I), could contribute to alkanes and cycloalkanes. Detailed three-dimensional collision cascades indicate "tube-like" energized zones inside the irradiated target, where this synthesis might take place. At higher doses and overlapping cascades, however, a stepwise synthesis through equations (6)–(8) might contribute to alkane/cycloalkane formation as well. Here, however, the inserting $CH_2$ must be suprathermal since no diffusion of thermal carbene at 10 K takes place (see § 4.2.2).

### 4.5. The Source of Suprathermal H and C Atoms

Based on our MARLOWE calculations, the elastic energy loss generates only 0.22 ± 0.04 H/0.07 ± 0.02 C (7.3 MeV H$^+$) and 3.17 ± 0.52 H/1.15 ± 0.25 C atoms (9.0 MeV $\alpha$) per impinging MeV particle in a 5 $\mu$m $CH_4$ target. As outlined in the previous paragraphs, suprathermal C atoms are crucial to synthesize C2 species; thermal radical recombination were found to play no role in these processes. A comparison of the number of knock-on carbon atoms with the sum of synthesized acetylene, ethylene, and ethane molecules, i.e., 1037 ± 340 (9.0 MeV $\alpha$) and 165 ± 78 (7.3 MeV H$^+$), clearly demonstrate that a second source of suprathermal C atoms besides direct knock-on particles must exist to account for the discrepancy between theory and experiment.

Hitherto, we contributed only to the elastic energy transfer generating suprathermal knock-on atoms and neglected inelastic processes. As mentioned above, the energy loss to
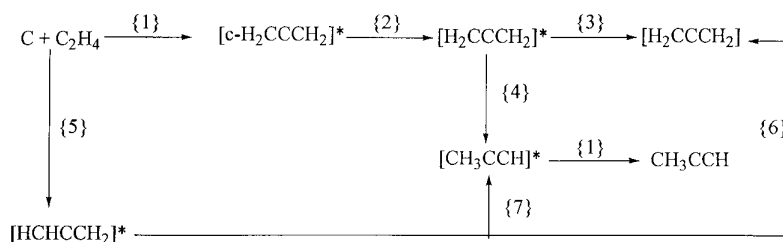


Fig. 13.—Compilation of mechanisms leading to formation of $C_3H_x$ species ($x = 4, 6, 8$)

the electronic system of the target and secondary electrons ionize single $CH_4$ molecules within a radius of about 50 Å perpendicular to the trajectory of the implanted ion. The stored potential energy, here via Coulomb interaction, can be released into kinetic energy of $CH_4^+$ fragments such as $C^+$, $CH^+$, as well as $CH_2^+$ (Roessler 1991) to result into additional, suprathermal species. As quoted above, these ions are neutralized prior to reaction and very likely represent the missing suprathermal C source.

### 4.6. *Comparison to Photolysis of* $CH_4$ *Targets*

A comparison of our MeV experiments with a recent study of UV photon processing of $CH_4$ ices at 10 K by Gerakines, Schutte, & Ehrenfreud (1997) offers further insights in the crucial role of suprathermal C atoms in hydrocarbon rich ices. These UV irradiation experiments indicate that 38% of the $CH_4$ was converted to methyl radicals (0.01%), C2 species ethylene (2.6%) and ethane (8%), the C3 species propane, and higher hydrocarbons holding structural units $R-CH_3$, $R-CH_2-R$, $R_2C=CH_2$, $R_2C=CRH$, as well as HCCR where " R " indicates an organic group. Most important neither acetylene, $C_2H_2$, nor vinyl radicals, $C_2H_3$, could be sampled. Since, however, $C_2H_2$ molecules were formed in our MeV irradiation through insertion of suprathermal carbon atoms and $C_2H_3$ via addition of H atoms to $C_2H_2$, we must conclude that UV exposure of $CH_4$ cannot generate suprathermal C atoms. Here UV photons interact in single quantum processes with a $CH_4$ molecule and are unable to ignite collision cascades to form suprathermal C atoms. In strong coincidence, Gerakines and coworkers postulated the formation of ethylene and ethane through reaction of UV photon-induced $CH_2$ and $CH_3$ radicals:

$$CH_2 + CH_4 \rightarrow C_2H_6 , \qquad (9)$$

$$CH_2 + CH_2 \rightarrow C_2H_4 , \qquad (10)$$

$$2\,CH_3 \rightarrow C_2H_6 . \qquad (11)$$
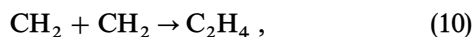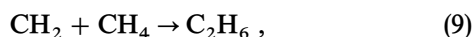
Since $CH_2$ as well as $CH_3$ are not mobile at 10 K, reactions (9)–(11) must be restricted to neighboring radicals in the UV-processed $CH_4$ targets.

### 5. ASTROPHYSICAL IMPLICATIONS

Our experiments demonstrate explicitly that MeV ion–induced suprathermal carbon atoms and nonequilibrium chemistry inside a single collision cascade present a powerful tool to synthesize a broad product spectrum from atomic and molecular hydrogen, H and $H_2$, via C2 species $C_2H_2$, $C_2H_3$, $C_2H_4$, $C_2H_5$, and $C_2H_6$, C3 species $CH_3CCH$, $H_2CCCH_2$, $C_3H_6$, and $C_3H_8$, as well as alkanes and polycyclic aromatic hydrocarbons (PAHs) as complex as coronene. The synthetic power of the implanted ions is even stronger as compared to UV photons since the last one cannot generate knock-on carbon atoms as well as collision cascades. Therefore, reactions in UV-processed samples are dominated by diffusion-limited reactions, e.g., equations (9)–(11), between neighboring radicals at 10 K. Suprathermal H atoms, however, can be generated in UV-irradiated samples as well considering a C–H bond energy of 4.4 eV in $CH_4$, and a UV photon of, e.g., 6.0 eV.

The versatile concept of suprathermal chemistry–induced formation of hydrocarbon molecules via insertion and addition of non-equilibrium C, CH, and $CH_2$ species as well as H abstraction processes elucidated from MeV irradiation of

$CH_4/CD_4$ model compounds could hold far-reaching consequences to "realistic" interstellar ices composed of $H_2O$, CO, $CH_3OH$, $NH_3$, $H_2S$, $CH_4$, $H_2CO$, OCS, $OCN^-$, $H_2$, and $CO_2$ (see § 1). As a typical example, we consider first the postulated synthetic route to interstellar methanol, $CH_3OH$, molecules on grain surfaces. Models assume a methanol synthesis through four successive H addition steps (reactions [11]–[14]) through the hydroxyformyl radical (11), formaldehyde/hydroxycarbene (12), and hydroxymethyl (13) on interstellar grains (Schutte et al. 1996, and references therein):

$$CO + H \rightarrow HCO , \qquad (11)$$

$$HCO + H \rightarrow H_2CO/HCOH , \qquad (12)$$

$$H_2CO/HCOH + H \rightarrow CH_2OH , \qquad (13)$$

$$CH_2OH + H \rightarrow CH_3OH . \qquad (14)$$
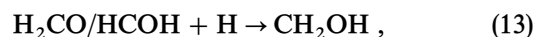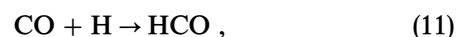
Recent laboratory work, however, indicates reaction (12) is too slow to form significant formaldehyde (Hiraoka et al. 1994). Suprathermal chemistry could resolve this puzzle: Galactic cosmic-ray particle induced nonequilibrium O and C atoms released in interstellar ice composita can insert into a C–H bond of $CH_4$ (eq. [15] below) and a O–H bond of a $H_2O$ molecule (eq. [16] below) to form an internally excited (*) methanol and formaldehyde as found in laboratory experiments (Schmitz, Nebeling, & Roessler 1987; Nebeling 1988):

$$O + CH_4 \rightarrow [CH_3OH^*] \rightarrow CH_3OH , \qquad (15)$$

$$C + H_2O \rightarrow [HCOH^*] \rightarrow [H_2CO^*] \rightarrow H_2CO . \qquad (16)$$
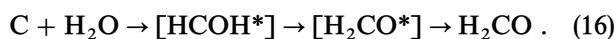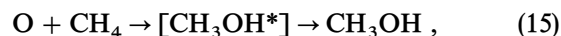
Since the excess energy can be released via phonon interaction with the solid target, the suprathermal pathway presents a *temperature-independent, one-step* reaction to form $H_2CO$ as well as $CH_3OH$ even at temperatures as low as 10 K. This approach is extendible to higher hydrocarbons as well, and insertion of suprathermal O into a C–H bond of ethane, $C_2H_6$, gives excited ethanol, $C_2H_5OH$, which could relax via phonon interaction as well:

$$O + C_2H_6 \rightarrow [C_2H_5OH^*] \rightarrow C_2H_5OH . \qquad (17)$$
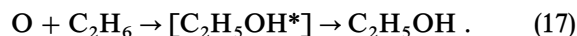
This solid state oxygen and carbon chemistry could represent a strong alternative to hitherto assumed diffusion controlled reactions on interstellar grain composita (Millar, Herbst, & Charnley 1991). Since the cosmic-ray particles induce not only suprathermal C and O atoms, but N and S atoms in interstellar ice composita as well, these suprathermal species react with molecules in the solid state, and an unprecedented product variety can be expected. It is worth mentioning that the cosmic-ray particle penetrates the micrometer-sized interstellar grain core, and suprathermal Fe, Mg, and Si atoms will be generated. These species offers unique synthetic power to form organometallic compounds. Once these molecules are formed on interstellar grains through suprathermal chemistry, equilibrium sublimation through heating of grains and their icy mantles by young stellar object embedded inside dense clouds, as well as explosive grain ejections of grains storing a critical concentration of radicals redistribute these newly formed molecules from the grains into the gas phase (d'Hendecourt et al. 1982).

Even an order of magnitude calculation shows that although the internal UV flux in dense, molecular clouds ($\phi = 10^3$ cm$^{-2}$ s$^{-1}$) ranges 2 orders of magnitude higher

than the cosmic-ray particle flux distribution maximum of $\phi = 10^1$ cm$^{-2}$ s$^{-1}$ for 1–10 MeV protons and $\alpha$-particles, each MeV particle can generate about 100 suprathermal species in a 0.2 $\mu$m thick icy layer and 0.3 $\mu$m thick grain core. The flux advantage of the internal UV field deep inside molecular clouds is clearly eliminated by the ability of a single MeV particle to induce collision cascades with up to 100 suprathermal species. Therefore, an opening from "photon-only universe" to process interstellar grains to include MeV ion synthesis is strongly encouraged.

## 6. SOLAR SYSTEM IMPLICATIONS

In our solar system, solid $CH_4$ was identifed unambiguously on Triton, Uranus, Neptune, Pluto and its moon Charon. Therefore, MeV ions as well as keV projectiles originating in the solar radiation field holding a flux $\phi = 2$–$3 \times 10^8$ cm$^{-2}$ s$^{-1}$ at 1 AU (AU = distance between Earth and Sun) are expected to modify these ices as well. Most important, the experimental identification of acetylene, $C_2H_2$, and ethane, $C_2H_6$, formed via suprathermal chemistry could resemble a pathway to form acetylene and ethane found in comet C/1996 B2 Hyakutake (Mumma et al. 1996; Mumma 1996; Hudson & Moore 1997).

## REFERENCES

Addepalli, V. B., & Rao, N. R. 1976, Indian J. Pure Appl. Phys., 14, 117
Alksne, Z. K., Alksnis, A. K., & Dzervits, U. K. 1991, Properties of Galactic Carbon Stars (Malabar: Orbit Books)
Allamandola, L. J., Sandford, S. A., & Valero, G. J. 1988, Icarus, 76, 225
Bellamy, L. J. 1968, Advances in Infrared Group Frequencies (London: Chapman & Hall)
Brown, W. L., Lanzerotti, L. J., & Johnson, R. E. 1982, Science, 218, 525
Chiar, J. E., Adamson, A. J., Kerr, T. H., & Whittet, D. C. B. 1994, ApJ, 426, 240
Cowieson, D. R., Barnes, A. J., Orville-Thomas, W. J., & Ram, J. 1981, Spectrosc., 10, 224
Cowley, C. R. 1985, An Introduction to Cosmochemistry (Cambridge: Cambridge Univ. Press)
d'Hendecourt, L. B., & Allamandola, L. J. 1986, A&AS, 64, 453
Dubrin, J., MacKay, C., & Wolfgang, R. 1964, J. Am. Chem. Soc., 86, 959
Geiss, J., et al. 1992, in COSPAR Colloq. Ser., Vol. 3, ed. E. Marsch & R. Schwenn (New York: Pergamon), 20
Gerakines, P. A., Schutte, W. A., & Ehrenfreud, P. 1996, A&A, 312, 289
Greenberg, J. M. 1971, A&A, 12, 240
Grigorev, E. I., Pshezhetskii, S. Y., & Trakhtenberg, L. I. 1985, Khimila Vysika Energika, 19, 41
Grim, R. J. A., & Greenberg, J. M. 1987, ApJ, 321, L91
Grim, R. J. A., Greenberg, J. M., de Groot, M. S., Baas, F., Schutte, W. A., & Schmitt, B. 1989, A&AS, 78, 191
Heyl, M. 1990, Rep. Jül-2409
Hiraoka, K., et al. 1994, Chem. Phys. Lett., 229, 408
Hollenbach, D. J., & Thronson, H. A. 1987, Interstellar Processes (Dordrecht: Reidel)
Hudson, R. L., & Moore, M. H. 1997, Icarus, in press
Johnson, R. E. 1990, Energetic Charged Particle Interactions with Atmospheres and Surfaces (Berlin: Springer)
Johnson, R. E., Lanzerotti, L. J., & Brown, W. L. 1984, Adv. Space Res., 4, 41
Kaiser, R. I., Gabrysch, A., Eich, G., & Roessler, K. 1997, ApJ, 484, 487 (Paper II)
Kaiser, R. I., Gabrysch, A., & Roessler, K. 1995, Rev. Sci. Instrum., 66, 3058
Kaiser, R. I., Jansen, P., Petersen, K., & Roessler, K. 1995, Rev. Sci. Instrum., 66, 5226
Kaiser, R. I., Lee, Y. T., & Suits, A. G. 1996, J. Chem. Phys., 105, 8705
Kaiser, R. I., & Roessler, K. 1997, ApJ, 475, 144 (Paper I)
Katz, R., Ackerson, B., Hormayoonfar, M., & Sharma, S. C. 1971, Radiation Res., 47, 402
Kondo, S., & Saeki, S. 1973, Spectrochim. Acta, A29, 1753
Lacy, J. H., Baas, F., Allamandola, L. J., Persson, S. E., McGregor, P. J., Lonsdale, C. J., Geballe, T. R., & van de Bult, C. E. P. 1984, ApJ, 276, 543

Lanzerotti, L. J., & Johnson, R. E. 1987, in Ion Beam Modifications of Insulators, ed. P. Mazzoldi & E. Arnold (Amsterdam: Elsevier), 631
MacKay, C., & Wolfgant, R. 1961, J. Am. Chem. Soc., 83, 2399
Millar, T. J., Herbst, E., & Charnley, S. B. 1991, ApJ, 369, 147
Moshammer, R. 1990, Ph.D. thesis, Fachhochschule Darmstadt
Mumma, M. J. 1996, Nature, 383, 581
Mumma, M. J., et al. 1996, Science, 272, 1310
Nebeling, B. 1988, Rep. Jülich 2245
Nyguist, I. M., Mills, I. M., Person, W. B., & Crawford, B. 1957, J. Chem. Phys., 26, 552
Palumbo, M. E., Tielens, A. G. G. M., & Tokunaga, A. T. 1995, ApJ, 449, 674
Pearl, J., Ngoh, M., Ospina, M., & Khanna, R. 1991, J. Geophys. Res., 96, 17477
Robinson, M. T. 1990, Nucl. Instrum. Meth., B67, 396
Roessler, K. 1991, in Solid-State Astrophysics, ed. E. Bussoletti & G. Strazzulla (Amsterdam: North-Holland)
Scheffler, H., & Elsässer, H. 1988, Physics of the Galaxy and Interstellar Matter (Berlin: Springer)
Schmitt, B. 1994, in AIP Conf. Proc., Molecules and Grains in Space, ed. I. Nenner (New York: AIP), 735
Schmitz, G., Nebeling, B., & Roessler, K. 1987, Rep. Jülich 2119
Schutte, W. A. 1998, in The Cosmic Dust Connection, ed. J. M. Greenberg (New York: AIP), in press
Schutte, W. A., et al. 1996, A&A, 309, 633
Schutte, W. A., Gerakines, P. A., Geballe, T. R., van Dishoeck, E. F., & Greenberg, J. M. 1996, A&A, 309, 633
Schutte, W. A., & Greenberg, J. M. 1997, A&A, in press
———. 1991, A&A, 244, 190
Shalabiea, O. M., & Greenberg, J. M. 1994, A&A, 290, 266
Simpson, J. A. 1983, in Introduction to the Galactic Cosmic Radiation, ed. R. Behrisch (Amsterdam: Reidel), 1
Smit, W. M. A., van Stalen, A. J., & Visser, T. 1978, J. Mol. Struct., 48, 177
Snelson, A. 1970, J. Phys. Chem., 74, 537
Stöcklin, G. 1969, Chemie heißer Atome (Weinheim: Verlag Chemie)
Taylor, K. K., Ache, H. J., & Wolf, A. P. 1975, J. Am. Chem. Soc., 97, 5970
Tegler, S. C., Weintraub, D. A., Rettig, T. W., Pendleton, Y. J., Whittet, D. C. B., & Kulesa, C. A. 1995, ApJ, 439, 279
Tielens, A. G. G. M., & Allamandola, L. J. 1987, in Interstellar Processes, ed. D. J. Hollenbach & H. A. Thronson (Dordrecht: Reidel), 397
Tielens, A. G. G. M., Tokunaga, A. T., Geballe, T. R., & Baas, F. F. 1991b, ApJ, 381, 181
Whittet, D. C. B. 1993, in Dust and Chemistry in Astronomy, ed. T. J. & D. A. Williams (Bristol: IOP Publ. Ltd.), 1
Wormhould, J., & McCurdy, K. E. 1989, Chem. Phys. Lett., 156, 47